

KfK 4567
Mai 1989

Thermodynamics of Ceramic Breeder Materials for Fusion Reactors

O. Götzmann
Institut für Material- und Festkörperforschung
Projekt Kernfusion

Kernforschungszentrum Karlsruhe

KERNFORSCHUNGSZENTRUM KARLSRUHE
Institut für Material- und Festkörperforschung
Projekt Kernfusion

KfK 4567

THERMODYNAMICS OF CERAMIC BREEDER MATERIALS FOR FUSION
REACTORS

O. Götzmann

Kernforschungszentrum Karlsruhe GmbH, Karlsruhe

Als Manuskript vervielfältigt
Für diesen Bericht behalten wir uns alle Rechte vor

Kernforschungszentrum Karlsruhe GmbH
Postfach 3640, 7500 Karlsruhe 1

ISSN 0303-4003

Thermodynamics of Ceramic Breeder Materials for Fusion Reactors

O. Götzmann

Abstract :

Based on known or deduced phase relationships in ternary lithium oxygen systems such as Li-Al-O, Li-Si-O and Li-Zr-O, the unknown free enthalpy of formation values of ternary compounds are calculated starting from the known data of the compounds of the binary border systems. Criterion for the data assessment is interconsistency of the data of all the compounds within a given multi-component system. With the help of these data the development of partial pressures during the breeding process can be calculated for all the compounds of interest. In order to facilitate a compatibility assessment the quaternary systems Cr-Li-Si-O, Fe-Li-Si-O and Be-Li-Si-O were also investigated and thermodynamic data of pertinent ternary and quaternary compounds determined.

Both the partial pressure development and the compatibility behaviour of a lithium containing compound are criteria for its qualification as a breeder material for a fusion reactor.

Thermochemie von keramischen Brutmaterialien für Fusionsreaktoren

O. Götzmann

Kurzfassung:

Ausgehend von bekannten oder hergeleiteten Phasenverhältnissen in ternären Lithium-Sauerstoff Systemen wie Li-AL-O, Li-Si-O und Li-Zr-O wurden die noch unbekanntene Werte der freien Bildungsenthalpie der ternären Verbindungen aus den bekannten Werten der Verbindungen der binären Randsysteme errechnet. Kriterium für die Berechnung ist die Konsistenz der Daten aller Verbindungen in einem Mehrkomponentensystem untereinander. Mit Hilfe dieser Daten kann die Partialdruckentwicklung der gewählten Brutmaterialien berechnet werden. Um das Verträglichkeitsverhalten abschätzen zu können, wurden auch die quaternären Systeme Cr-Li-Si-O, Fe-Li-Si-O und Be-Li-Si-O untersucht und die thermochemischen Daten der dazugehörigen ternären und quaternären Verbindungen bestimmt.

Sowohl die Partialdruckentwicklung wie auch das Verträglichkeitsverhalten von Lithiumverbindungen sind Kriterien bei der Auswahl von Brutmaterialien für Fusionsreaktoren.

1. Introduction

Lithium-containing oxide ceramics are being considered as tritium breeder materials in the blanket of nuclear fusion reactors. These compounds are primarily silicates, aluminates and zirconates of lithium. For an evaluation of their behaviour under operational conditions, thermochemical data such as the free enthalpies of formation can be very helpful. However, there exists up to now very little useful thermodynamic data for the complex oxides of lithium. In this report thermodynamic data were generated by utilizing the little data that exists, following the general rules of chemical thermodynamics and making some plausible assumptions. The data produced have to satisfy two criteria which will be stated later.

All of the ceramic breeder materials under consideration are compounds of ternary chemical systems. If the ternary phase diagram of the respective system is known, one can easily, in a first step, write a set of chemical equations involving all the compounds in the system. If there is no phase diagram available a plausible one is made up with the little data that exists. From the set of chemical reactions, one gets a set of inequalities involving the free enthalpy values of the ternary compounds. This set of inequalities constitute the first criterion.

"This work has been performed in the framework of the Nuclear Fusion Project of the Kernforschungszentrum Karlsruhe and is supported by the European Communities within the European Fusion Technology Program."

2. Li-Al-O

The ternary phase diagrams of the three chemical systems, which this report deals with, are fairly simple as can be shown by the phase diagram of the Li-Al-O system (fig. 1). Lithium as well as the other metal partners have practically only one oxidation state, which means that the ternary compound formation takes place only on the tie line between Li_2O and the binary oxide of the partners. In fig. 1. it is on the tie line between Li_2O and Al_2O_3 . There are four ternary compounds in the Li-Al-O system reported in the literature: Li_5AlO_4 , Li_3AlO_3 , LiAlO_2 and LiAl_5O_8 . Li_3AlO_3 decomposes above 700 K. It will not be considered any further in this report. So we have to deal with 3 ternary compounds, and for the situation on the tie line Li_2O - Al_2O_3 , one can write three chemical reactions:

1. $2\text{Li}_2\text{O} + \text{LiAlO}_2 = \text{Li}_5\text{AlO}_4$
2. $\text{Li}_5\text{AlO}_4 + \text{LiAl}_5\text{O}_8 = 6\text{LiAlO}_2$
3. $\text{LiAlO}_2 + 2\text{Al}_2\text{O}_3 = \text{LiAl}_5\text{O}_8$

The resulting inequalities are (criterion 1):

1. $\Delta G_f^\circ(\text{Li}_5\text{AlO}_4) - 2\Delta G_f^\circ(\text{Li}_2\text{O}) - \Delta G_f^\circ(\text{LiAlO}_2) < 0$
2. $6\Delta G_f^\circ(\text{LiAlO}_2) - \Delta G_f^\circ(\text{Li}_5\text{AlO}_4) - \Delta G_f^\circ(\text{LiAl}_5\text{O}_8) < 0$
3. $\Delta G_f^\circ(\text{LiAl}_5\text{O}_8) - \Delta G_f^\circ(\text{LiAlO}_2) - 2\Delta G_f^\circ(\text{Al}_2\text{O}_3) < 0$

The values for the binary oxides are known [1]. Also known is the free enthalpy of formation for the metaaluminate (LiAlO_2) [2]. So we get for each of the two unknown values a range within to look for the right value.

For the application of the second criterion we have to define the phase relationships below the Li_2O - Al_2O_3 tie line (see fig. 1), i.e., in the region Li-Li₂O-Al₂O₃-Al. With the approximate values for Li_5AlO_4 from the first criterion and the value for LiAl [3], it follows that the phase relationships in this region are those shown in fig. 1 (i. e., a tie exists between Li and Li_5AlO_4 but not between Li_2O and LiAl). With the phase relationship established we can deduce the potential drift, which means that according to this diagram the oxygen

potential in the Li-Al-O system is lowest in the Li-Li₅AlO₄-LiAl field. It will increase towards Al/Al₂O₃ and also toward Li/Li₂O. The formulation of this potential drift constitutes the second criterion. The oxygen potential in the Li/Li₂O-field is known. The one in the next field and in the following fields are calculated according to the following formulae:

1. $2\mu_{O_2}(1) = \Delta G_f^\circ(\text{Li}_5\text{AlO}_4) - \Delta G_f^\circ(\text{LiAl})$
2. $2\mu_{O_2}(2) = \Delta G_f^\circ(\text{Li}_5\text{AlO}_4) - 5\Delta G_f^\circ(\text{LiAl})$
3. $3\mu_{O_2}(3) = 5\Delta G_f^\circ(\text{LiAlO}_2) - \Delta G_f^\circ(\text{Li}_5\text{AlO}_4)$
4. $3\mu_{O_2}(4) = \Delta G_f^\circ(\text{LiAl}_5\text{O}_8) - \Delta G_f^\circ(\text{LiAlO}_2)$

The oxygen potential in the field of Al/Al₂O₃ is also known.

For the established phase diagram of the Li-Al-O system, the second criterion requires that:

$$\mu_{O_2}(1) < \mu_{O_2}(2) < \mu_{O_2}(3) < \mu_{O_2}(4) < \mu_{O_2}(\text{Al/Al}_2\text{O}_3)$$

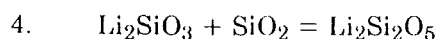
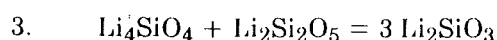
$$\text{and } \mu_{O_2}(1) < \mu_{O_2}(\text{Li/Li}_2\text{O})$$

The values for the equilibrium oxygen potentials, which were chosen for $\mu_{O_2}(1)$ through $\mu_{O_2}(4)$ are shown fig. 2. The corresponding free enthalpy of formation values for the ternary compounds that satisfy both criteria are given in Table I

3. Li-Si-O

The Li-Si-O system was treated likewise. Ternary compounds exist only on the tie-line Li₂O-SiO₂ (fig. 3). Four compounds are reported in the literature: Li₈SiO₆, Li₄SiO₄, Li₂SiO₃ and Li₂Si₂O₅. The most lithiumrich compound, Li₈SiO₆, decomposes at 1100 K. With these 4 ternary compounds we can write 4 chemical reactions:

1. $2\text{Li}_2\text{O} + \text{Li}_4\text{SiO}_4 = \text{Li}_8\text{SiO}_6$ T < 1100 K
2. $\text{Li}_8\text{Si}_4 + 2\text{Li}_2\text{SiO}_3 = 3\text{Li}_4\text{SiO}_4$ T < 1100 K



According to the first criterion we obtain four inequalities:

$$1. \quad \Delta G_f^\circ(\text{Li}_8\text{SiO}_6) - 2\Delta G_f^\circ(\text{Li}_2\text{O}) - \Delta G_f^\circ(\text{Li}_4\text{SiO}_4) < 0 \quad T < 1100 \text{ K}$$

$$2. \quad 3\Delta G_f^\circ(\text{Li}_4\text{SiO}_4) - \Delta G_f^\circ(\text{Li}_8\text{SiO}_6) - 2\Delta G_f^\circ(\text{Li}_2\text{SiO}_3) < 0 \quad T < 1100 \text{ K}$$

$$3. \quad 3\Delta G_f^\circ(\text{Li}_2\text{SiO}_3) - \Delta G_f^\circ(\text{Li}_4\text{SiO}_4) - \Delta G_f^\circ(\text{Li}_2\text{Si}_2\text{O}_5) < 0$$

$$4. \quad \Delta G_f^\circ(\text{Li}_2\text{Si}_2\text{O}_5) - \Delta G_f^\circ(\text{Li}_2\text{SiO}_3) - \Delta G_f^\circ(\text{SiO}_2) < 0$$

For temperatures above 1100 K, only three reactions can be written which yield three inequalities. Reactions (1) and (2) are replaced by



and the corresponding inequality reads:

$$1a) \quad \Delta G_f^\circ(\text{Li}_4\text{SiO}_4) - \Delta G_f^\circ(\text{Li}_2\text{O}) - \Delta G_f^\circ(\text{Li}_2\text{SiO}_3) < 0 \quad T > 1100 \text{ K}$$

Thermochemical data for all the lithium silicates could be found in the literature [2,4]. A first estimation showed that a tie-line between Li and the lithium rich silicates does not exist, a fact which makes this system easier for application of the second criterion. The lowest oxygen potential is that of the Li/Li₂O-equilibrium and the highest that for the Si/SiO₂ equilibrium. For simplicity's sake, the various binary Li-Si compounds were combined in one compound, Li₂Si. This simplification does not introduce a major error in the thermochemical treatment of the system.

So, for the phase diagram given in fig. 3, the equilibrium oxygen potentials in the phase fields below the Li₂O-SiO₂ tie line can be calculated with the following expressions:

$$\mu_{\text{O}_2}(1) = 2/3 [\Delta G_f^\circ(\text{Li}_8\text{SiO}_6) - 3\Delta G_f^\circ(\text{Li}_2\text{O}) - \Delta G_f^\circ(\text{Li}_2\text{Si})] \quad T < 1100 \text{ K}$$

$$\mu_{O_2}(2) = 1/3 [3\Delta G_f^\circ(\text{Li}_4\text{SiO}_4) - \Delta G_f^\circ(\text{Li}_8\text{SiO}_6) - 2\Delta G_f^\circ(\text{Li}_2\text{Si})] \quad T < 1100 \text{ K}$$

$$\mu_{O_2}(3) = 1/2 [\Delta G_f^\circ(\text{Li}_4\text{SiO}_4) - 2\Delta G_f^\circ(\text{Li}_2\text{Si})]$$

$$\mu_{O_2}(4) = 2\Delta G_f^\circ(\text{Li}_4\text{SiO}_3) - \Delta G_f^\circ(\text{Li}_4\text{SiO}_4)$$

$$\mu_{O_2}(5) = \Delta G_f^\circ(\text{Li}_2\text{Si}_2\text{O}_5) - \Delta G_f^\circ(\text{Li}_2\text{SiO}_3)$$

For temperatures above 1100 K, the equations for $\mu_{O_2}(1)$ and $\mu_{O_2}(2)$ are replaced by:

$$\mu_{O_2}(1a) = 2/3 [\Delta G_f^\circ(\text{Li}_4\text{SiO}_4) - \Delta G_f^\circ(\text{Li}_2\text{O}) - \Delta G_f^\circ(\text{Li}_2\text{Si})] \quad T > 1100 \text{ K}$$

The second criterion requires now that:

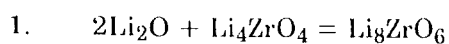
$$\mu_{O_2}(1) < \mu_{O_2}(2) < \mu_{O_2}(3) < \mu_{O_2}(4) < \mu_{O_2}(5) < \mu_{O_2}(\text{Si}/\text{SiO}_2)$$

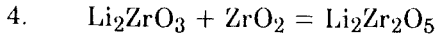
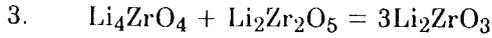
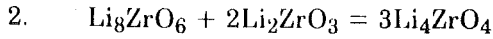
$$\text{and } \mu_{O_2}(1) \text{ or } \mu_{O_2}(1a) > \mu_{O_2}(\text{Li}/\text{Li}_2\text{O})$$

The equilibrium oxygen potentials chosen for $\mu_{O_2}(1)$ through $\mu_{O_2}(5)$ are shown in fig. 4. The corresponding values for the free enthalpies of formation for the ternary compounds are given in Table 1. The value for the metasilicate found in the literature [2] was taken as correct, the values for the others were adjusted in a way that they satisfied both criteria.

4. Li-Zr-O

The treatment of Li-Zr-O required more effort than the two previous systems. There are five ternary compounds reported in the literature for this system: Li_8ZrO_6 , Li_4ZrO_4 , $\text{Li}_6\text{Zr}_2\text{O}_7$, Li_2ZrO_3 and $\text{Li}_2\text{Zr}_2\text{O}_5$. Two of them, Li_4ZrO_4 and $\text{Li}_6\text{Zr}_2\text{O}_7$, are said to be alternative [5], i.e, they describe alternative compositions of the same compound. If Li_4ZrO_4 is considered, the phase diagram is that given in fig. 5 and for the four ternary compounds on the Li_2O - ZrO_2 tie line one can write four reactions:





The stability criterion (criterion 1) requires that:

$$1. \quad \Delta G_f^\circ(\text{Li}_8\text{ZrO}_6) - 2\Delta G_f^\circ(\text{Li}_2\text{O}) - \Delta G_f^\circ(\text{Li}_4\text{ZrO}_4) < 0$$

$$2. \quad 3\Delta G_f^\circ(\text{Li}_4\text{ZrO}_4) - 2\Delta G_f^\circ(\text{Li}_2\text{ZrO}_3) - \Delta G_f^\circ(\text{Li}_8\text{ZrO}_6) < 0$$

$$3. \quad 3\Delta G_f^\circ(\text{Li}_2\text{ZrO}_3) - \Delta G_f^\circ(\text{Li}_4\text{ZrO}_4) - \Delta G_f^\circ(\text{Li}_2\text{Zr}_2\text{O}_5) < 0$$

$$4. \quad \Delta G_f^\circ(\text{Li}_2\text{Zr}_2\text{O}_5) - \Delta G_f^\circ(\text{Li}_2\text{ZrO}_3) - \Delta G_f^\circ(\text{ZrO}_2) < 0$$

Besides the binary oxides, free enthalpy of formation data for the metazirconate (Li_2ZrO_3) is also available [2]. A rough evaluation of the phase relationships in the lithium-rich corner with the help of the results from the stability criterion indicates that while there is no tie line between Li_2O and Zr one does exist between Li and a lithium-rich oxide compound. This means that the Li/ Li_2O equilibrium does not establish the lowest oxygen potential in a phase field in equilibrium with an oxide compound.

However, the greater difficulty in treating this system arises from the fact that zirconium metal has a rather large solubility for oxygen. Therefore, the equilibrium oxygen potential cannot be calculated from the free enthalpy of formation of ZrO_2 .

For the phase diagram in fig. 5, the equilibrium oxygen potentials in the phase fields below the Li_2O - ZrO_2 tie line can be calculated with the following expressions:

$$\mu_{\text{O}_2} (1) = \frac{2}{6-x} [\Delta G_f^0(\text{Li}_8\text{ZrO}_6) - \Delta G_f^0(\text{ZrO}_x)]$$

$$\mu_{\text{O}_2} (2) = \frac{2}{2-x} [2\Delta G_f^0(\text{Li}_4\text{ZrO}_4) - \Delta G_f^0(\text{Li}_8\text{ZrO}_6) - \Delta G_f^0(\text{ZrO}_x)]$$

$$\mu_{O_2} (3) = \frac{2}{2-x} [2\Delta G_f^0(\text{Li}_2\text{ZrO}_3) - \Delta G_f^0(\text{Li}_4\text{ZrO}_4) - \Delta G_f^0(\text{ZrO}_x)]$$

$$\mu_{O_2} (4) = \frac{2}{2-x} [2\Delta G_f^0(\text{Li}_2\text{Zr}_2\text{O}_5) - \Delta G_f^0(\text{Li}_2\text{ZrO}_3) - \Delta G_f^0(\text{ZrO}_x)]$$

$$\mu_{O_2} (5) = \frac{2}{1.58} [2\Delta G_f^0(\text{ZrO}_2) - \Delta G_f^0(\text{ZrO}_{0.42})]$$

In these expressions x is the O/Zr ratio pertaining to the corresponding equilibrium phase field. In the (last) field in equilibrium with ZrO_2 it reaches its highest value which corresponds to the saturation level of oxygen in α -zirconium. For the temperature range considered, the saturation solubility of oxygen in zirconium metal reaches 29 to 30 at %, which corresponds to a O/Zr ratio of 0.42.

Again the second consistency criterion requires that:

$$\mu_{O_2}(1) < \mu_{O_2}(2) < \mu_{O_2}(3) < \mu_{O_2}(4) < \mu_{O_2}(5)$$

$$\text{and } \mu_{O_2}(1) < \mu_{O_2}(\text{Li/Li}_2\text{O})$$

To determine these oxygen potentials, it is necessary to know the relationship between oxygen potential and oxygen content in metallic zirconium. There are two references in the literature. Kubaschewski and Dench [6] determined the oxygen potential for several oxygen contents at 1000°C (1273 K). Komarek and Silver [7] made measurements in the temperature range from 1000 to 1300 K and determined the oxygen potential from approximately 1 to 30 at % of oxygen in α -zirconium and its temperature dependence. There is a large discrepancy between the two sets of data and there is also a large discrepancy between the partial values given by Komarek and Silver and the accepted integral values of the free enthalpy of formation for zirconium oxide listed in thermodynamic data tables [1,2,3]. Therefore, a general relationship for the oxygen potential, the free enthalpies of formation, and the oxygen content of zirconium-oxygen alloys was established. This was done with the help of the graphical method to determine integral values from partial values. Fig. 6 shows the development of the oxygen potential as a function of the O/Zr ratio in the Zr-O system (fat line). The oxygen potential curve is composed of two sections: a one-phase region, and a two-phase region. In the two-phase region the oxygen potential is constant over $0.42 < \text{O/Zr} \leq 2$ and corresponds to the formation potential of ZrO_2 . In the one-phase region, extending from $x = 0$ to $x = 0.42$, the oxygen potential is more

negative by an amount which is a function of x . This function of x was chosen, as is usually the case in thermodynamics, as a logarithmic function. The oxygen potential in the one-phase region is composed of:

$$\mu_{O_2}(ZrO_x) = \mu_{O_2}(ZrO_2) + 2A \cdot \ln \frac{x}{x_0}$$

where $x = O/Zr$, $x_0 = 0.42$ (saturation oxygen content) and A is a constant independent of x .

Integration along $\mu_{O_2}(ZrO_x)$ in the one-phase region reads:

$$\Delta G_f^0(ZrO_x) = 1/2 \int_0^x \mu_{O_2}(ZrO_x) dx = 1/2 \int_0^x \mu_{O_2}(ZrO_2) dx + A \int_0^x \ln \frac{x}{x_0} dx$$

After integration we obtain:

$$\Delta G_f^0(ZrO_x) = \frac{x}{2} \mu_{O_2}(ZrO_2) + A \left(x \cdot \ln \frac{x}{x_0} - x \right)$$

If the integration of $\mu_{O_2}(ZrO_x)$ is done from

$x = 0$ up to $x = 2$ we obtain:

$$\Delta G_f^0(ZrO_2) = \mu_{O_2}(ZrO_2) - A \cdot x_0$$

Since $\Delta G_f^0(ZrO_2)$ and x_0 are known we only need to find the value for the oxygen potential of the ZrO_2 -formation to be able to calculate all the values necessary for the second criterion. Unfortunately, it was not available.

There is a specific value of x , which shall be named x_c , at which the numerical values of $\Delta G_f^0(ZrO_2)$ and $\mu_{O_2}(ZrO_x)$ are the same:

$$\mu_{O_2}(ZrO_{x_c}) = \Delta G_f^0(ZrO_2) = \mu_{O_2}(ZrO_2) + 2A \ln \frac{x_c}{x_0}$$

With the two expressions for $\Delta G_f^0(ZrO_2)$ equated we obtain:

$$A \cdot x_0 = -2A \ln \frac{x_c}{x_0}$$

For $x_0 = 0.42$ we get

$$x_c = 0.34$$

So for an O/Zr ratio of 0.34 we know the oxygen potential, no matter what the value of the constant A is. We would need only one more value of the oxygen potential at another O/Zr ratio to determine A for a given temperature. The expression for A and its temperature dependence then was chosen such that the oxygen potential varied with temperature and oxygen concentration in a way similar to that found by Komarek and Silver [7], however at a higher level to make the partial values consistent with the accepted integral values for ZrO_2 .

The value chosen for A is:

$$A = 55\,000 + 14.3 T \text{ [J]}$$

It turned out that the value for the oxygen potential at oxygen saturation given by Kubaschewski and Dench [6] needs only a slight correction to be consistent with the set of data produced with this value for A.

Introducing A into the proper equations, the molar partial and integral free enthalpies can be calculated with the following formulae:

$$\mu_{O_2}(ZrO_2) = -1\,074\,900 + 193 T \text{ [J]}$$

$$\mu_{O_2}(ZrO_x) = \mu_{O_2}(ZrO_2) + 2(55\,000 + 14.3 T) \ln \frac{x}{x_0} \text{ [J]}$$

$$\Delta G_f^0 (\text{ZrO}_x) = \frac{x}{2} \mu_{\text{O}_2} (\text{ZrO}_2) + (55\,000 + 14.3 T) \left(x \cdot \ln \frac{x}{x_0} - x \right) \text{ |J|}$$

Formally, all the ΔG_f^0 values, except those for the ternary compounds, that are needed to calculate the equilibrium oxygen potentials in the Li-Zr-O system are now available. The oxygen potentials determined are shown in fig. 7. Values for the free enthalpies of formation of the ternary Li-Zr-O compounds that satisfy both criteria are given in Table 1.

5. Development of partial pressures

The advantage of having thermochemical data is the possibility to make predictions about the behaviour of materials. One field of predictions for ceramic breeder materials is their evaporation behaviour or, to be more exact, the development of partial pressures of gaseous species that are being produced during operation.

During the breeding process, lithium is transformed to tritium, chemically that means hydrogen, and the oxygen which was bound to the lithium is liberated. This causes an increase in oxygen potential in the breeder material. In all probability, oxygen and tritium will react with each other to form water (T_2O). Water formation will drastically impede tritium diffusion and release from the breeder material. Oxygen, hydrogen, and lithium will produce various volatile species which will be in chemical equilibrium with the breeder material. The equilibrium situation is dependent on the oxygen potential. Fig. 8 gives an example of how the partial pressures of the various gaseous species are influenced by the oxygen potential in breeder blankets of lithium silicates. At a low oxygen potential the major gaseous species is atomic lithium. Its pressure decreases, however, with increasing oxygen potential. The hydroxides are abundant only at high oxygen potentials. Fig. 8 shows the situation for an assumed hydrogen pressure of 10^{-3} atm. Gaseous lithium oxides do not contribute significantly to the vaporisation of these materials even at high oxygen potentials for temperatures up to 1200 K.

Tritium will be present predominantly as water in and on the blanket material at oxygen potentials higher than -400 kJ at an operating temperature of 1000 K. If the tritium is to stay predominantly nonoxidized, which would certainly greatly

increase its mobility and decrease its retention, the oxygen potential in the material has to be kept low. This can be achieved by introducing a getter which buffers the oxygen potential at a sufficiently low level.

Fig. 9 and 10 show in a similar representation the pressure development in the Li-Al-O and Li-Zr-O system, respectively. Comparing the three systems on their volatilization behaviour one will find out that for the same temperature and potential conditions the silicates generate marginally lower pressures than the aluminates, whereas the zirconates produce the highest ones. This comparison is demonstrated again in fig. 11 by using the partial pressures of LiOH in equilibrium with a water pressure of 10^{-4} atm and the metacompounds of the three material groups. Metasilicate has the lowest LiOH pressure. The advantage of the silicates is even more demonstrated by the LiOH pressure in equilibrium with the orthosilicate (Li_4SiO_4) which is not higher than the one in equilibrium with metazirconate. The orthocompounds, which are richer in lithium, produce higher pressures than the metacompounds.

The pressure values obtained by vaporisation of the lithium compounds reported in the literature are much different from those given here. The partial pressures measured by mass spectrometry of vaporized materials are dissociation pressures, whereas those given here are equilibrium pressures for fixed potentials. The dissociation pressures can also be calculated with the free enthalpy of formation values given in this report. However, the data generated thus far are for operational temperatures (600 -1200 K); the vaporization measurements, on the other hand, are always made at higher temperatures (>1300 K). Hence, a set of free enthalpy of formation values had to be produced which are valid for a higher temperature range in order to be able to calculate dissociation pressures that can be compared with those reported in the literature. This set of data is given in Table 2. The calculated lithium and oxygen dissociation pressures for the compounds of the Li-Si-O, Li-Al-O and Li-Zr-O systems are shown in fig. 12, 13 and 14, respectively. A comparison among the three systems again shows that the zirconates yield the highest pressures.

Compatibility

Another aspect of operational behaviour which can be evaluated with thermochemical data is compatibility. Of interest is the compatibility of candidate breeder materials with stainless steel and beryllium. Stainless steels

are considered as cladding and structural materials in the breeder blanket. Beryllium is in discussion as a neutron multiplier. Hence, additional ternary systems to be considered to supply reliable thermochemical data for a compatibility evaluation are Li-Cr-O, Li-Fe-O and Li-Be-O. The respective phase diagrams for the temperature range of 600 to 1200 K are shown in figs. 15 through 17. The free enthalpy of formation values for ternary compounds that are consistent with these phase diagrams are given in table 3. Also given in this table are values of compounds existing in quaternary systems composed of Li-Si-O and Cr, Fe, and Be, respectively.

In case of incompatibility of the ceramic breeder materials with stainless steel or beryllium, the possible interaction products could be simple oxides or complex lithium based oxides. If we compare the formation oxygen potentials of the breeder materials with those of possible reaction products in fig. 18 we see that oxygen exchange reactions are not likely to take place with stainless steels. They can, however, occur with beryllium. The only breeder material that is likely not to oxidize beryllium is Li_5AlO_4 . Thermodynamically, the compounds of low lithium content are least desirable since they have the higher dissociation oxygen potential. However, they involve essentially solid reaction products, whereas the lithium-rich materials produce low melting lithium compounds or alloys. Hence, due to kinetic reasons, compounds low in lithium could be less aggressive towards beryllium than the theoretically more compatible lithium-rich compounds.

Even though possible reaction products of ceramic breeder materials and stainless steel components have a higher formation oxygen potential than the breeder materials, a good compatibility during operation is not insured. Tritium breeding involves an increase in oxygen potential in the breeder blanket. Oxidation of stainless steel then becomes possible with the help of lithium which overcomes the stainless steel passivation by forming lithium complex oxides. For these reactions, both the potentials of lithium and oxygen are responsible and the reaction probability is best expressed by the potential (or activity) of lithium oxide (since it is a Li_2O -complex which is exchanged). Fig. 19 gives the lithium oxide potential for the ceramic breeder materials and for possible stainless steel reaction products.

The most likely reaction product is LiCrO_2 . The probability of its formation decreases with decreasing lithium content of the breeder material. The zirconates are more likely to corrode stainless steel than the silicates and aluminates. Iron

will form reaction products with lithium rich compounds only except for the meta- and even dizirconate which both exhibit ferrate formation probabilities.

7. Conclusions

Values for the free enthalpies of formation of all the known ternary compounds in the systems Li-Si-O, Li-Al-O and Li-Zr-O were calculated based on the known values of the compounds of the binary border systems and the known value of one ternary compound in each system. The values were checked for consistency with a given ternary phase diagram by employing consistency criteria. The resulting thermodynamic values were used to demonstrate the operational behaviour of the prospective breeder materials. Based on the predicted behaviour, the silicates have the best potential and the zirconates the least for use as fusion breeder materials.

Literature

- [1] L.B. Pankratz:
Thermodynamic Properties of Elements and Oxides, U.S. department of the Interior, Bureau of Mines, 1982
- [2] JANAF Thermochemical Tables, NSRD-NBS-37, 1974 Supplement
- [3] I. Barin, O. Knacke:
Thermochemical Properties of Inorganic Substances, Springer-Verlag Berlin Heidelberg New York, 1973 and Supplement 1977
- [4] T. B. Lindemer, t.M. Besmann, C. E. Johnson:
Thermodynamic Review and Calculations - Alkali-Metal Oxide Systems with Nuclear Fuels, Fission Products, and Structural Materials, J. Nucl. Mater. 100 (1981) 178-226
- [5] ASTM file Nr. 34-312
- [6] O. Kubaschewski, W.A. Dench:
J. Inst. Metals, 84 (1955-56) 440
- [7] K. L. Komarek, M. Silver:
in: Thermodynamics of Nuclear Materials, IAEA, 1962, 749
- [8] O. Kubaschewski, E. LL. Evans, C. B. Alcock:
Metallurgical Thermochemistry, 4th Ed., 1974,
Pergamon Press, Oxford, New York, Toronto, Sydney

Table 1: Free enthalpy of formation values for temperatures between 600 and 1200 K [J/mole]

		Ref.
Li ₂ O	-60400 + 138 T	/1/
SiO ₂	-904000 + 173 T	/1/
Al ₂ O ₃	-1680000 + 320 T	/1/
ZrO ₂	-1097100 + 187 T	/1/
Li ₂ SiO ₃	-1656500 + 321 T	/2/
LiAlO ₂	-1196000 + 222 T	/2/
Li ₂ ZrO ₃	-1766500 + 323 T	/3/
Li ₄ SiO ₄	-2328000 + 472 T	/3/ a
Li ₂ Si ₂ O ₅	-2578000 + 494 T	/2/ a
Li ₈ SiO ₆	-3556000 + 176 T	d
Li ₅ AlO ₄	-2563000 + 490 T	d
LiAl ₅ O ₈	-4580000 + 850 T	d
Li ₂ Zr ₂ O ₅	-2878700 + 513 T	d
Li ₄ ZrO ₄	-2385600 + 450 T	d
Li ₈ ZrO ₆	-3608000 + 700 T	d
LiAl	-53400 + 20 T	d
Li ₂ Si	-8200 + 25 T	/3/

d = determined, a = adjusted

Table 2: Free enthalpy of formation values for temperatures between 1200 and 1600 K [J/mole].

			Ref.
Li ₂ O	-597700 + 133 T		/1/
Al ₂ O ₃	-1690000 + 329 T		/1/
SiO ₂	-901200 + 171 T		/1/
ZrO ₂	-10910000 + 182 T		/1/
LiAlO ₂	-1196700 + 223 T		/2/
Li ₅ AlO ₄	-2548000 + 480 T		d
LiAl ₅ O ₈	-4604000 + 870 T		d
Li ₂ ZrO ₃	-1753500 + 312 T		/3/
Li ₂ Zr ₂ O ₅	-2860000 + 497 T		d
Li ₄ ZrO ₄	-2366600 + 434 T		d
Li ₈ ZrO ₆	-3577000 + 674 T	1200 < T < ~1400 K	d
Li ₂ SiO _{3,s}	-1649600 + 315 T	1200 < T < 1480 K	/2/
Li ₂ SiO _{3,l}	-1613200 + 290 T	1480 ≅ T < 1600 K	/2/
Li ₂ SiO _{3,l}	-1789000 + 400 T	1600 < T ≅ 1700 K	/2/
Li ₄ SiO ₄	-2313000 + 462 T	1200 ≅ T < 1530 K	d
Li ₂ Si ₂ O ₅	-2562000 + 483 T	1200 ≅ T < 1300 K	d

s = solid, l = liquid, d = determined

Table 3: Free enthalpy of formation values for possible incompatibility products [J/mole] valid for temperatures from 600 to 1200 K.

Cr ₂ O ₃	-1131000 + 255 T	/1/
FeO	-268900 + 62 T	/1/
Fe ₂ O ₃	-811500 + 250 T	/1/
Fe ₃ O ₄	-1096000 + 303 T	/1/
FeCr ₂ O ₄	-1406680 + 306 T	/1,8/
Fe ₂ SiO ₄	-1470100 + 317 T	/1,8/
NiO	-236000 + 86 T	/1/
NiCr ₂ O ₄	-1420200 + 349 T	/1,8/
LiCrO ₂	-950000 + 190 T	/4/ a
LiFeO ₂	-727700 + 183 T	/3/
Li ₅ FeO ₄	-1957000 + 462 T	/4/ a
LiFe ₅ O ₈	-2370650 + 685 T	/4/ a
LiCrSi ₂ O ₆	-2848000 + 544 T	d
Li ₂ CrO ₄	-1394000 + 346 T	/4/ a
Li ₃ CrO ₄	-1669000 + 391 T	/4/ a
Li ₂ Si	-82000 + 25 T	d
FeSi	-78000 - 17,4 T	3
Cr ₃ Si ₂	-136000 - 10 T	3
BeO	-608000 + 97 T	/1/
Be ₂ SiO ₄	-2130000 + 370 T	/3/ a
Li ₂ Bi ₂ O ₃	-1832000 + 334 T	d
Li ₂ BeSiO ₄	-2290000 + 420 T	d

a = adjusted, d = determined

Figures

- Fig. 1:** Phase diagram of the Li-Al-O system for 700 to 1200 K.
- Fig. 2:** Oxygen potential for the formation of compounds in the Li-Al-O system.
- Fig. 3:** Phase diagram of the Li-Si-O system for 600 to 1200 K.
- Fig. 4:** Oxygen potential for the formation of compounds in the Li-Si-O system.
- Fig. 5:** Phase diagram of the Li-Zr-O system for 600 to 1200 K.
- Fig. 6:** Oxygen potential in the Zr-O system as function of the O/Zr ratio.
- Fig. 7:** Oxygen potential for the formation of compounds in the Li-Zr-O system.
- Fig. 8:** Pressure development of gaseous species over Li-Si-O compounds in dependence of the oxygen potential at 1000 K. Partial pressures for Li_2 , LiH , Li_2O and $(\text{LiOH})_2$ are given only for Li_4SiO_4 .
- Fig. 9:** Pressure development of gaseous species over Li-Al-O compounds in dependence of oxygen potential at 1000 K. Partial pressures for Li_2 , LiH , Li_2O and $(\text{LiOH})_2$ are given only for Li_5AlO_4 .
- Fig. 10:** Pressure development of gaseous species over Li-Zr-O compounds in dependence of the oxygen potential at 1000 K. Partial pressures for Li_2 , LiH , Li_2O and $(\text{LiOH})_2$ are given only for Li_8ZrO_6 .
- Fig. 11:** Comparison of pressure development in the three breeder material groups by the partial pressure of LiOH over the metacompounds at a water vapour pressure of 10^{-4} atm. The pressure over orthosilicate is also shown to demonstrate the relatively good behaviour of the silicates.
- Fig. 12:** Dissociation pressures of lithium and oxygen over lithium compounds in the Li-Si-O system. $p_0 = 1 \text{ atm} = 101325 \text{ Pa}$.
- Fig. 13:** Dissociation pressures of lithium and oxygen over lithium compounds in the Li-Al-O system. $p_0 = 1 \text{ atm} = 101325 \text{ Pa}$.
- Fig. 14:** Dissociation pressures of lithium and oxygen over lithium compounds in the Li-Zr-O system. $p_0 = 1 \text{ atm} = 101325 \text{ Pa}$.
- Fig. 15:** Phase diagram of the Li-Cr-O system and cross section level $\text{Li}_2\text{O-Cr}_2\text{O}_3\text{-SiO}_2$ for the quaternary Cr-Li-Si-O system for 600 to 1200 K.
- Fig. 16:** Phase diagram of the Li-Fe-O system and cross section level $\text{Li}_2\text{O-Fe}_2\text{O}_3\text{-SiO}_2$ for the quaternary Fe-Li-Si-O system for 600 to 1200 K.
- Fig. 17:** Phase diagram of the Li-Be-O system and cross section level $\text{Li}_2\text{O-BeO-SiO}_2$ for the quaternary Be-Li-Si-O system for 600 to 1200 K.
- Fig. 18:** Oxygen potential of formation of ceramic compounds.
- Fig. 19:** Potential of Li_2O of ceramic materials.

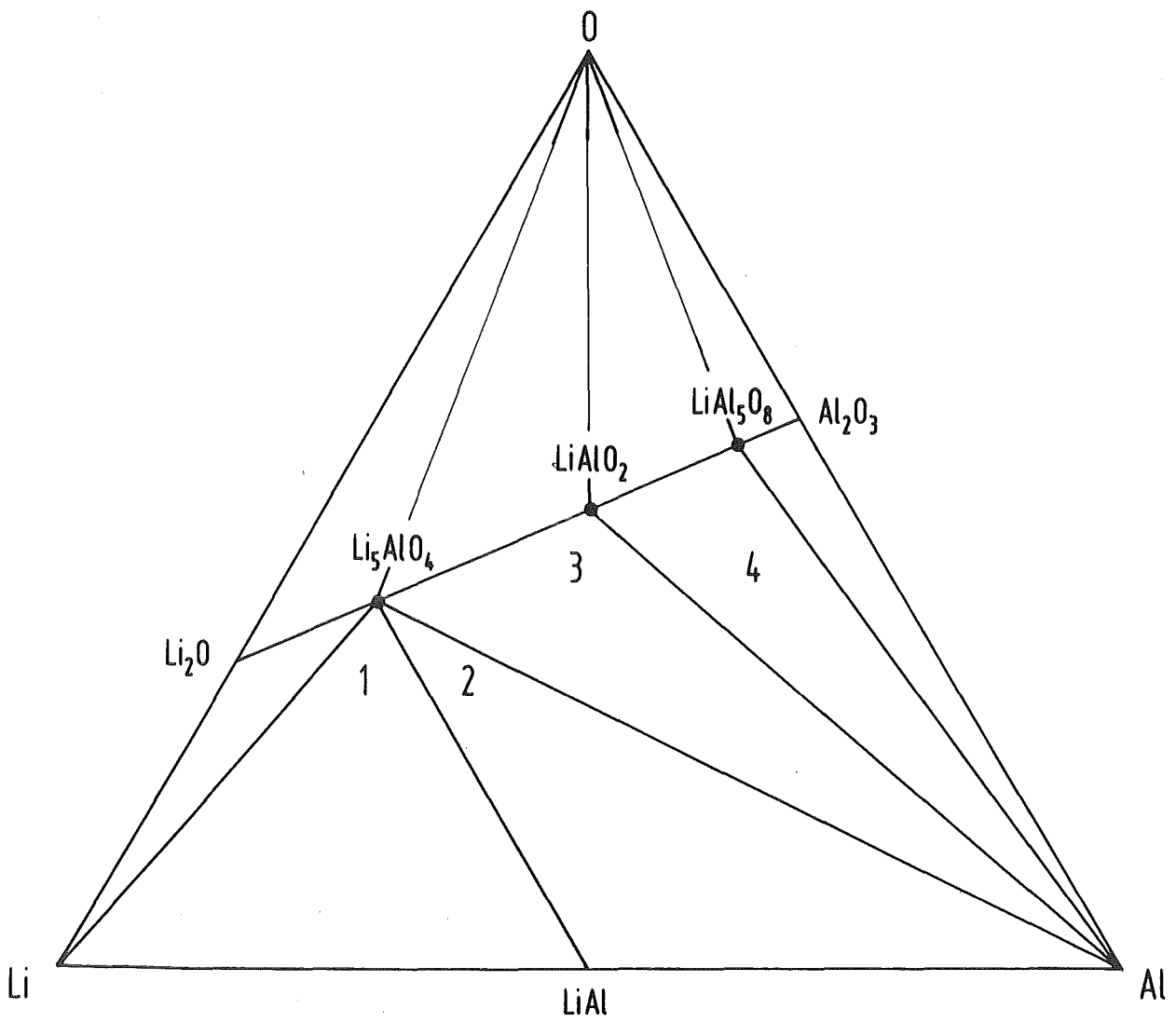


Fig. 1: Phase diagram of the Li-Al-O system for 700 to 1200 K.

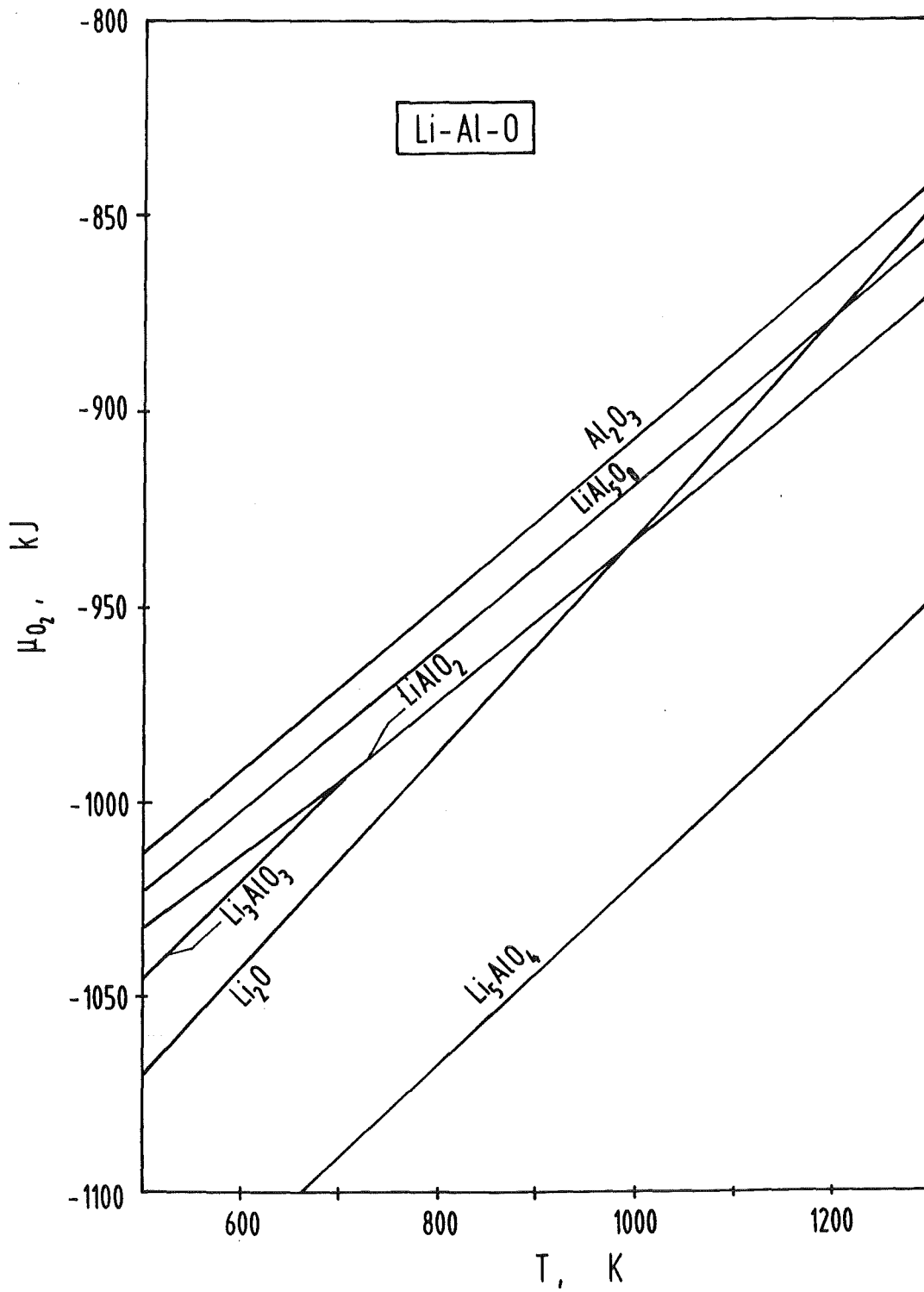


Fig. 2: Oxygen potential for the formation of compounds in the Li-Al-O system.

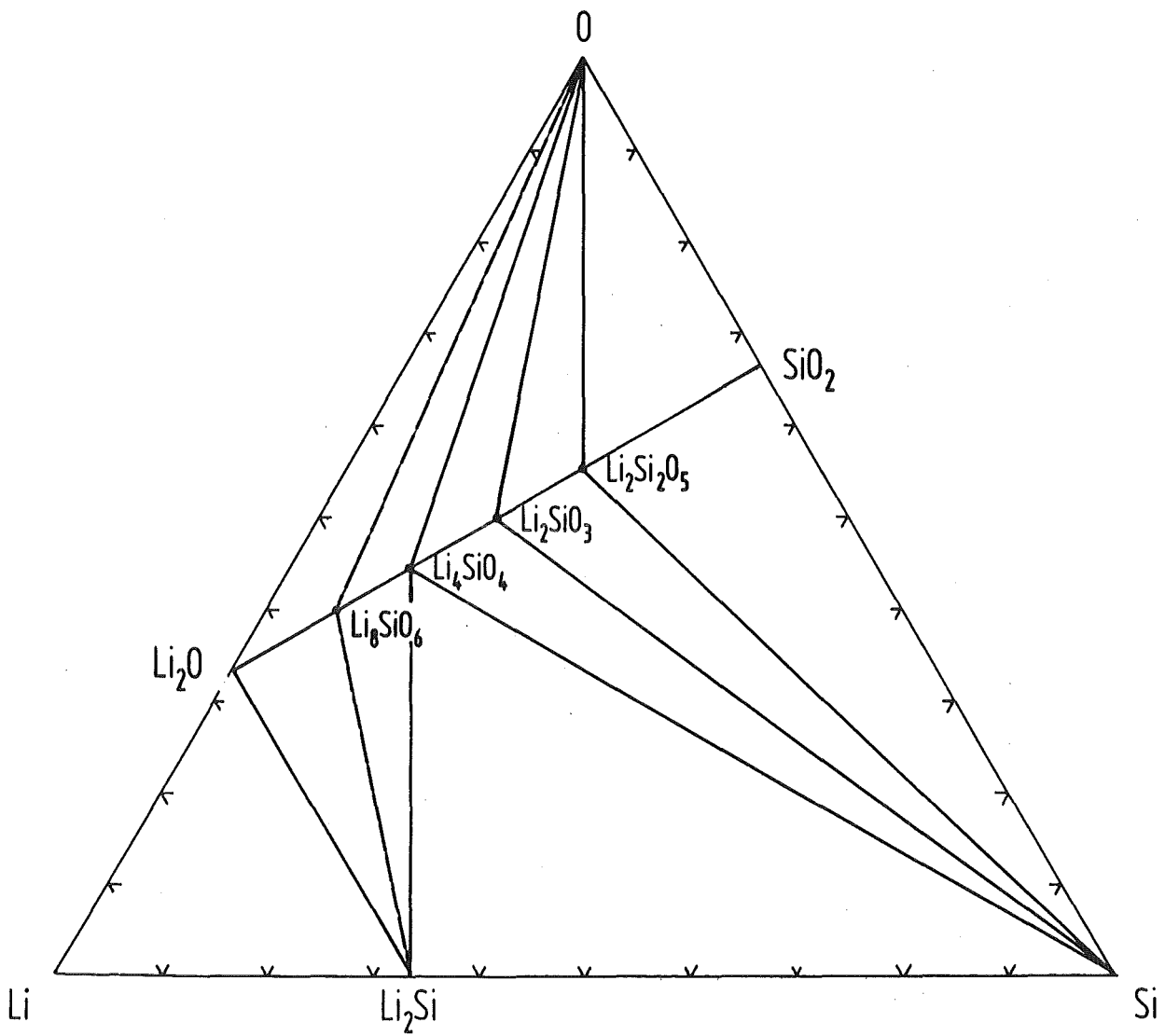


Fig. 3: Phase diagram of the Li-Si-O system for 600 to 1200 K.

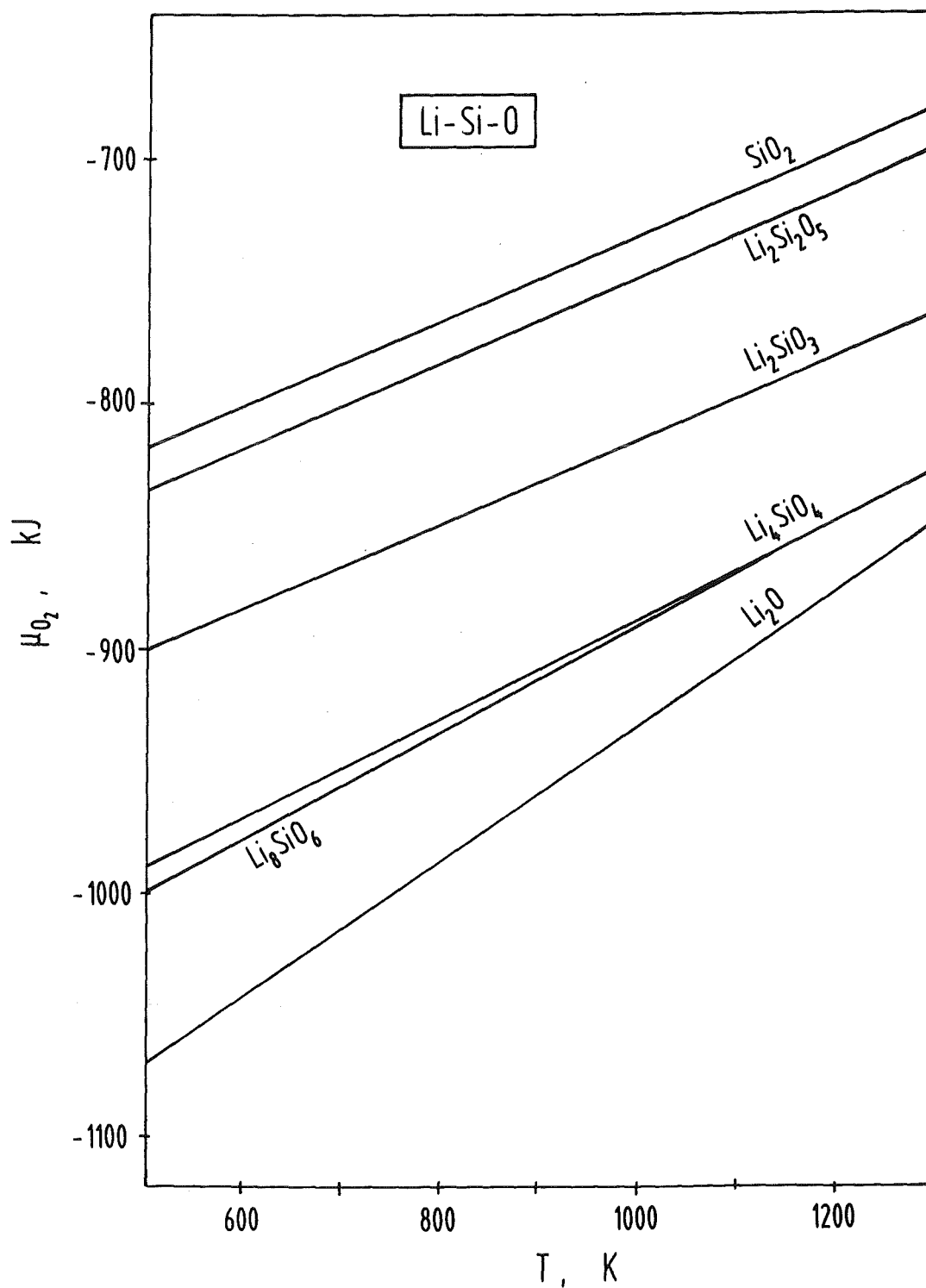


Fig. 4: Oxygen potential for the formation of compounds in the Li-Si-O system.

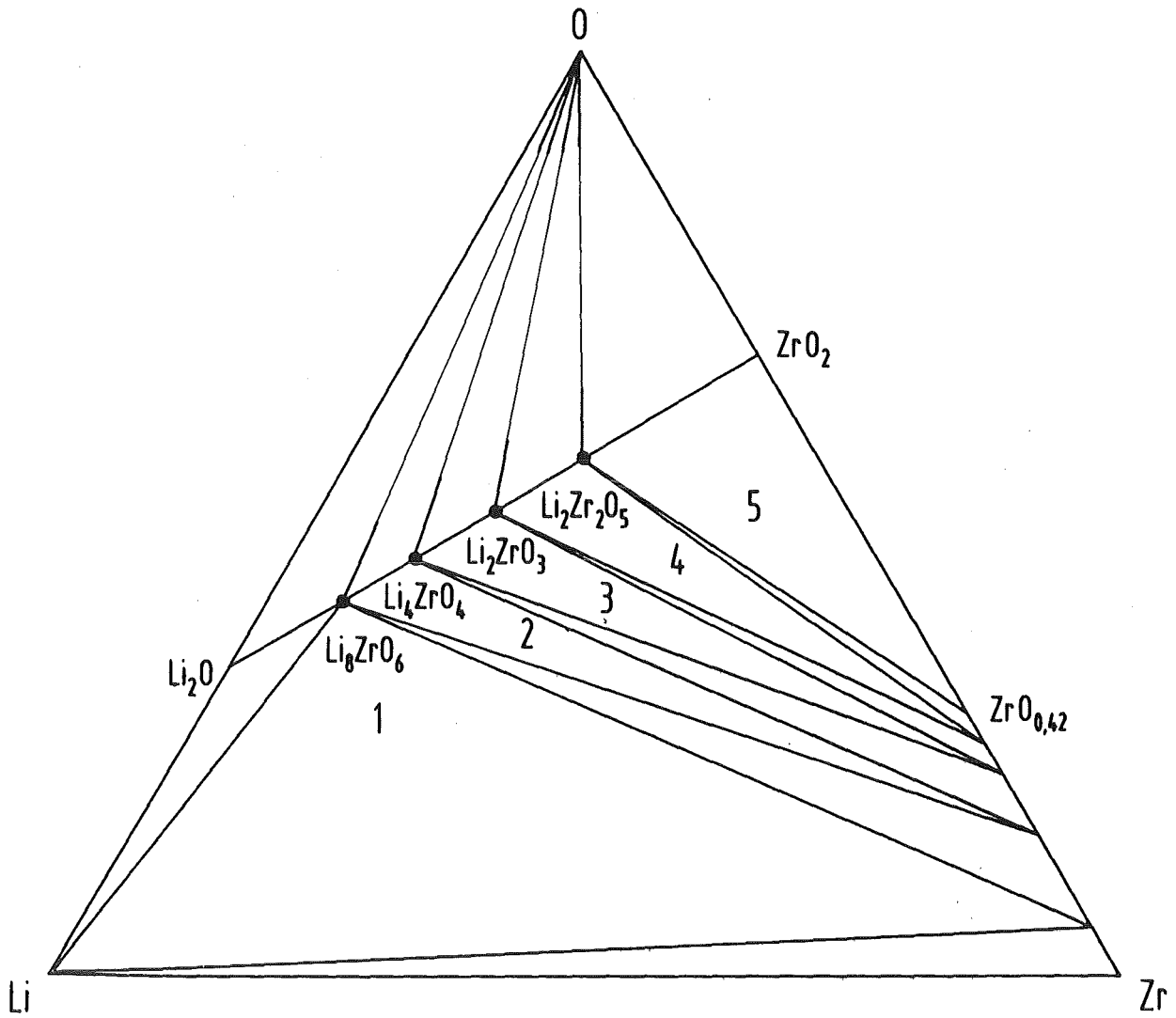


Fig. 5: Phase diagram of the Li-Zr-O system for 600 to 1200 K.

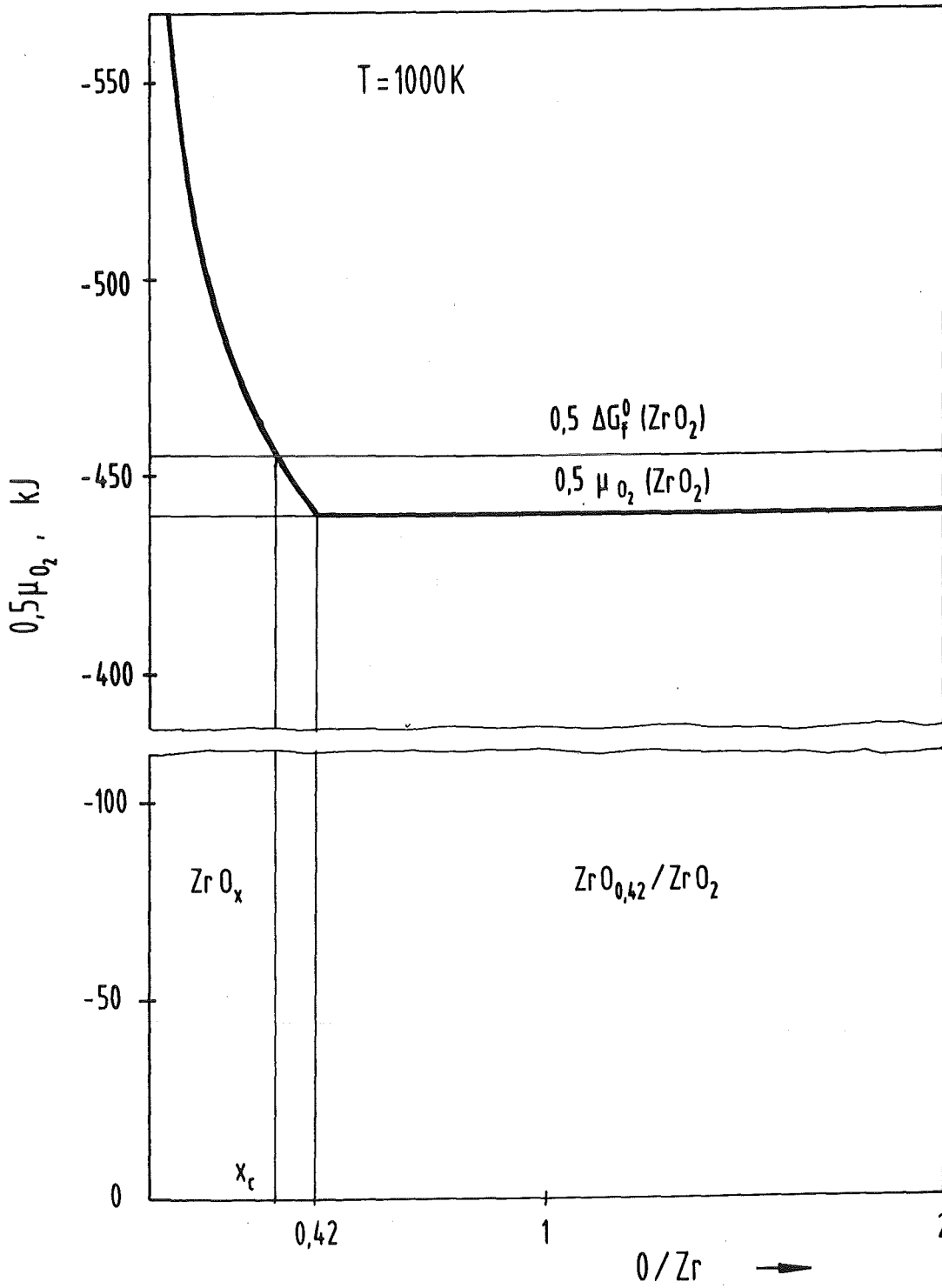


Fig. 6: Oxygen potential in the Zr-O system as function of the O/Zr ratio.

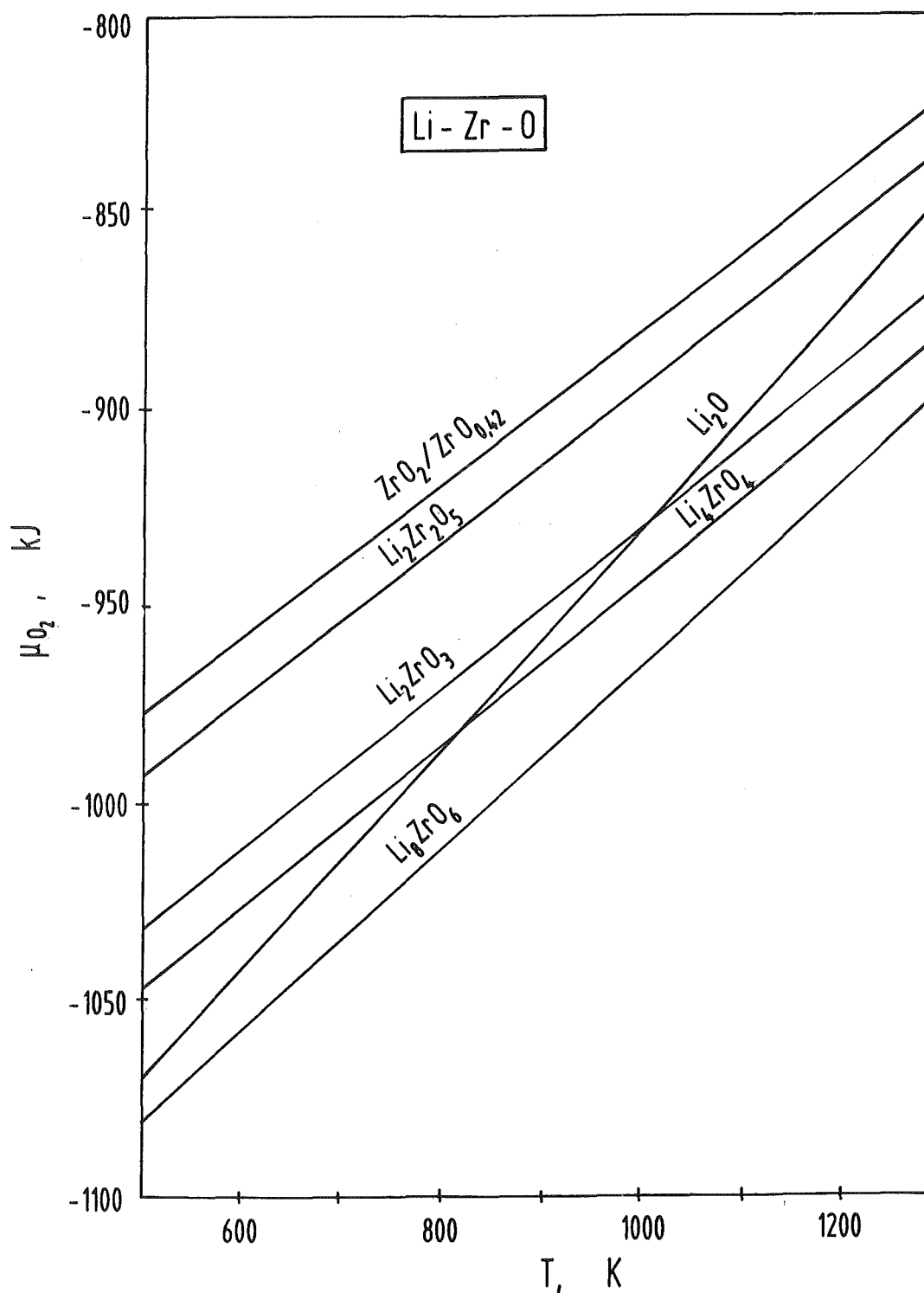


Fig. 7: Oxygen potential for the formation of compounds in the Li-Zr-O system.

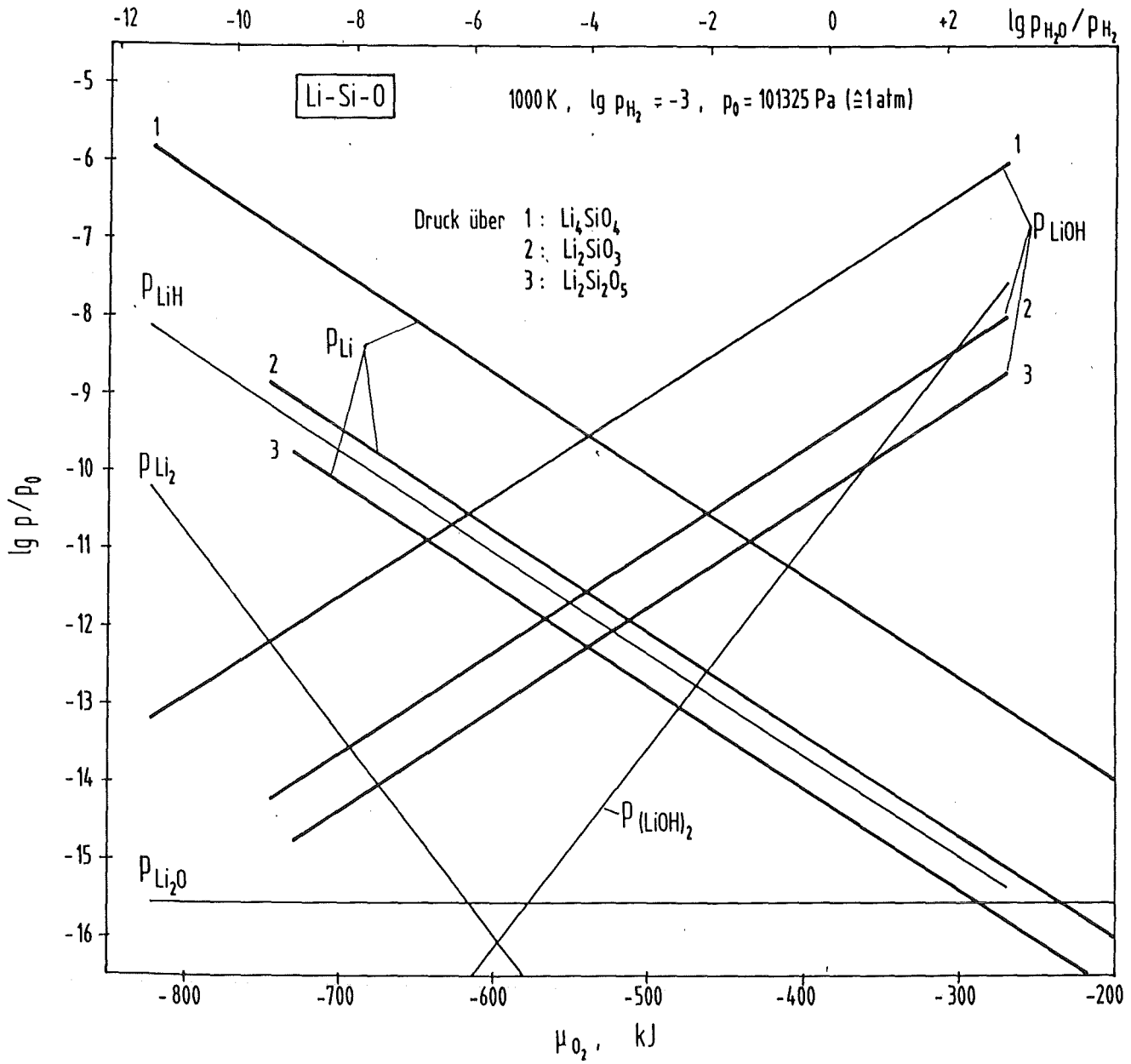


Fig. 8: Pressure development of gaseous species over Li-Si-O compounds in dependence of the oxygen potential at 1000 K. Partial pressures for Li_2 , LiH , Li_2O and $(\text{LiOH})_2$ are given only for Li_4SiO_4 .

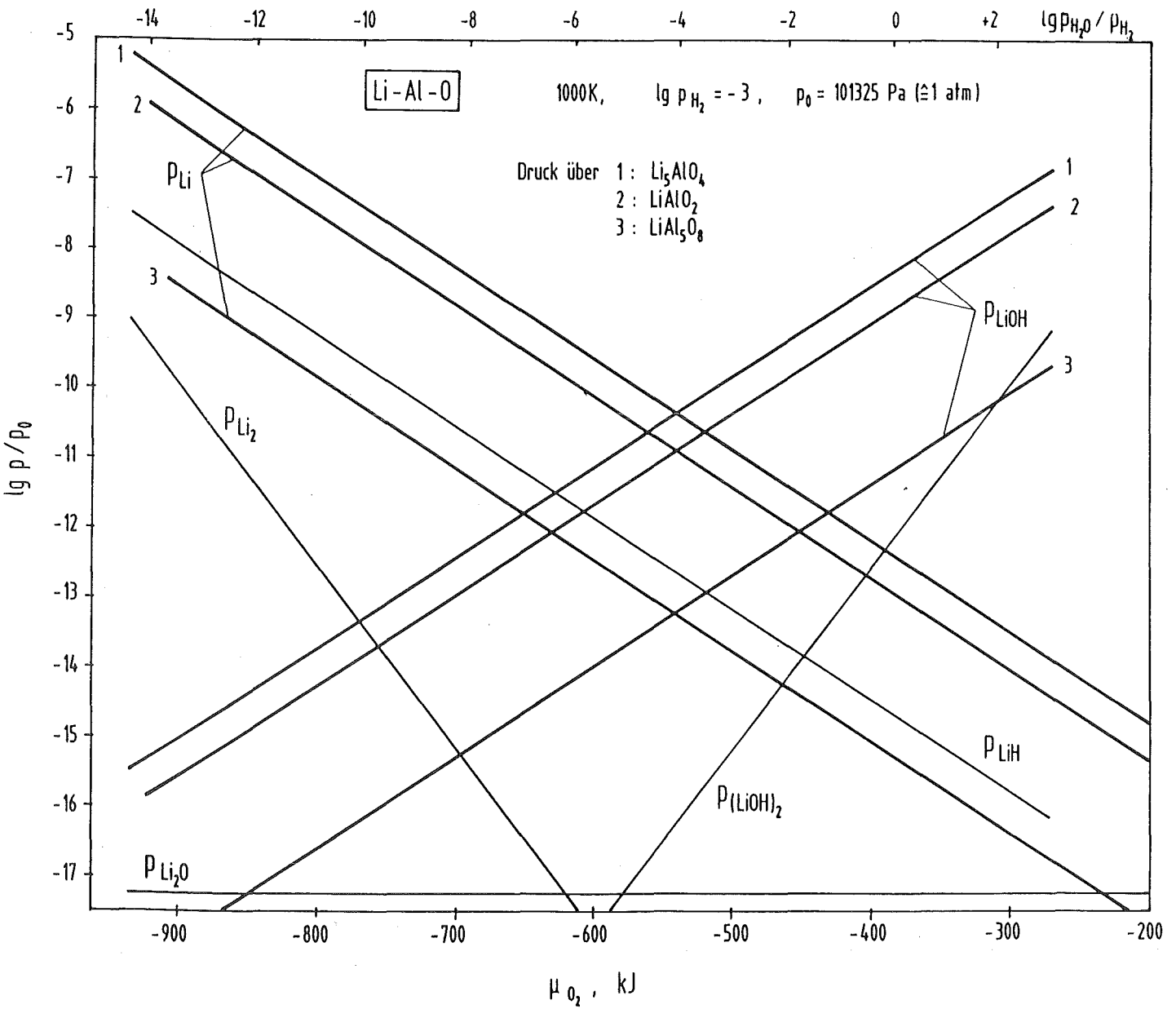


Fig. 9: Pressure development of gaseous species over Li-Al-O compounds in dependence of oxygen potential at 1000 K. Partial pressures for Li_2 , LiH , Li_2O and $(\text{LiOH})_2$ are given only for Li_5AlO_4 .

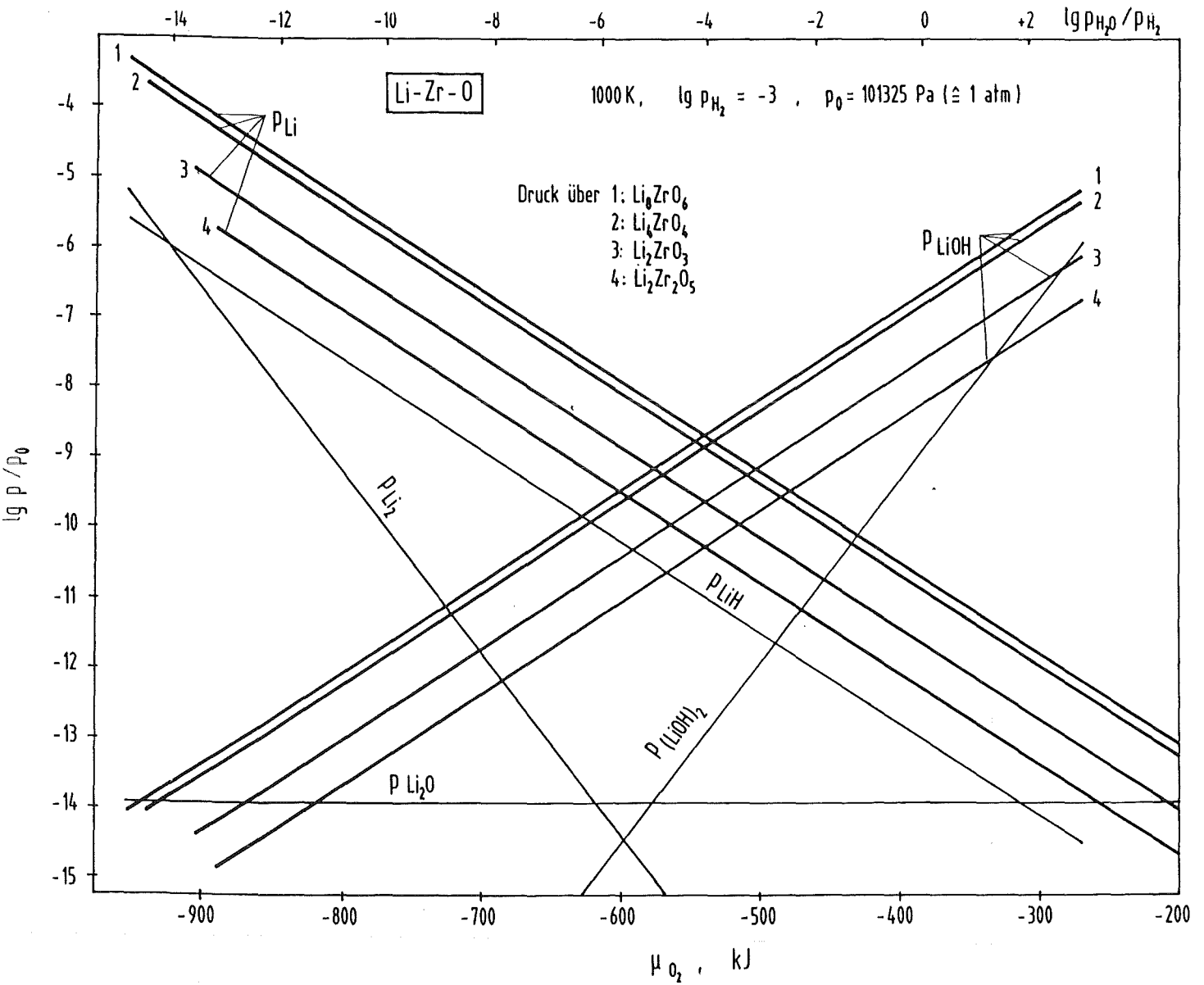


Fig. 10: Pressure development of gaseous species over Li-Zr-O compounds in dependence of the oxygen potential at 1000 K. Partial pressures for Li_2 , LiH , Li_2O and $(\text{LiOH})_2$ are given only for Li_9ZrO_6 .

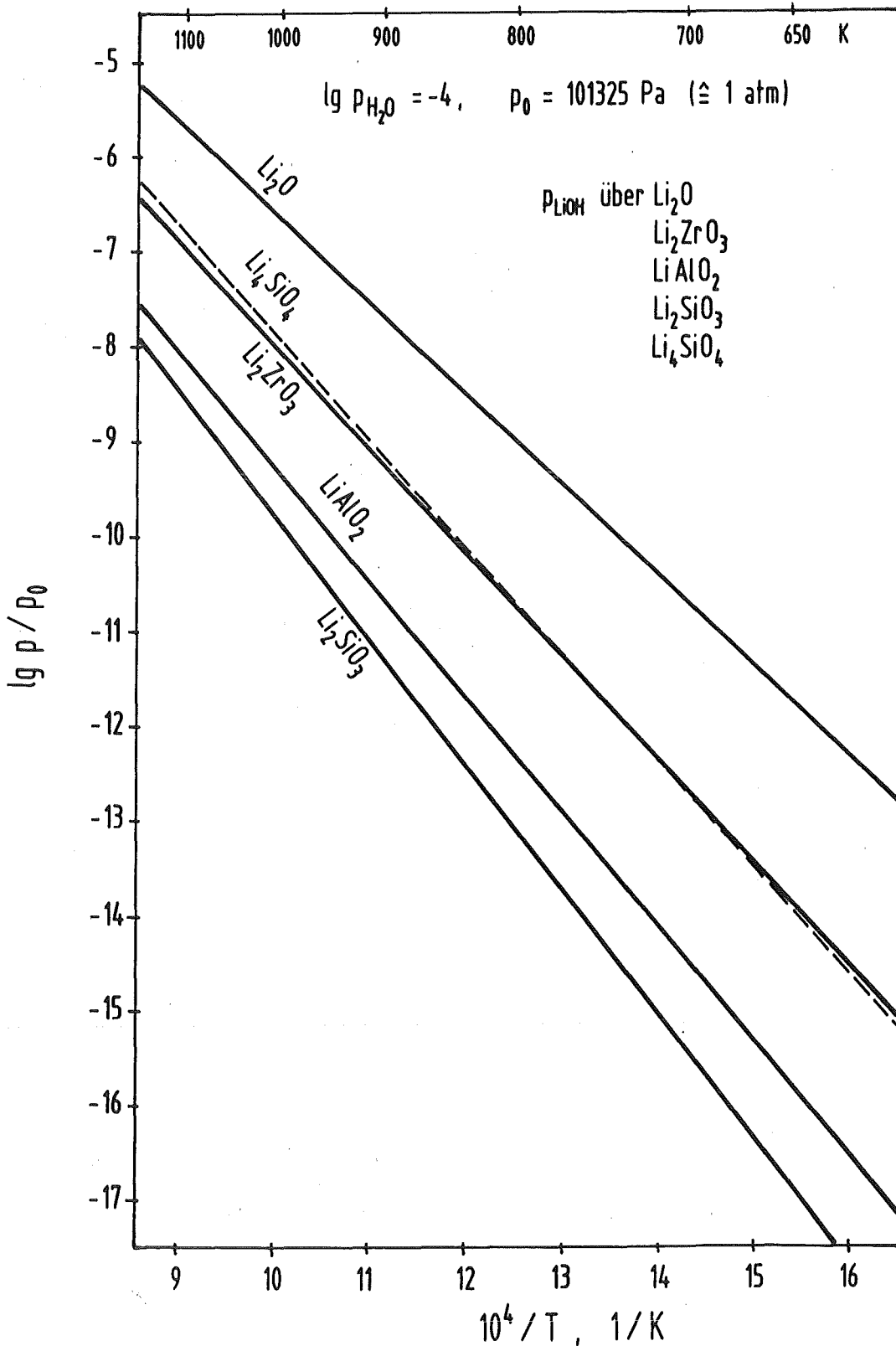


Fig. 11: Comparison of pressure development in the three breeder material groups by the partial pressure of LiOH over the metacompounds at a water vapour pressure of 10^{-4} atm. The pressure over orthosilicate is also shown to demonstrate the relatively good behaviour of the silicates.

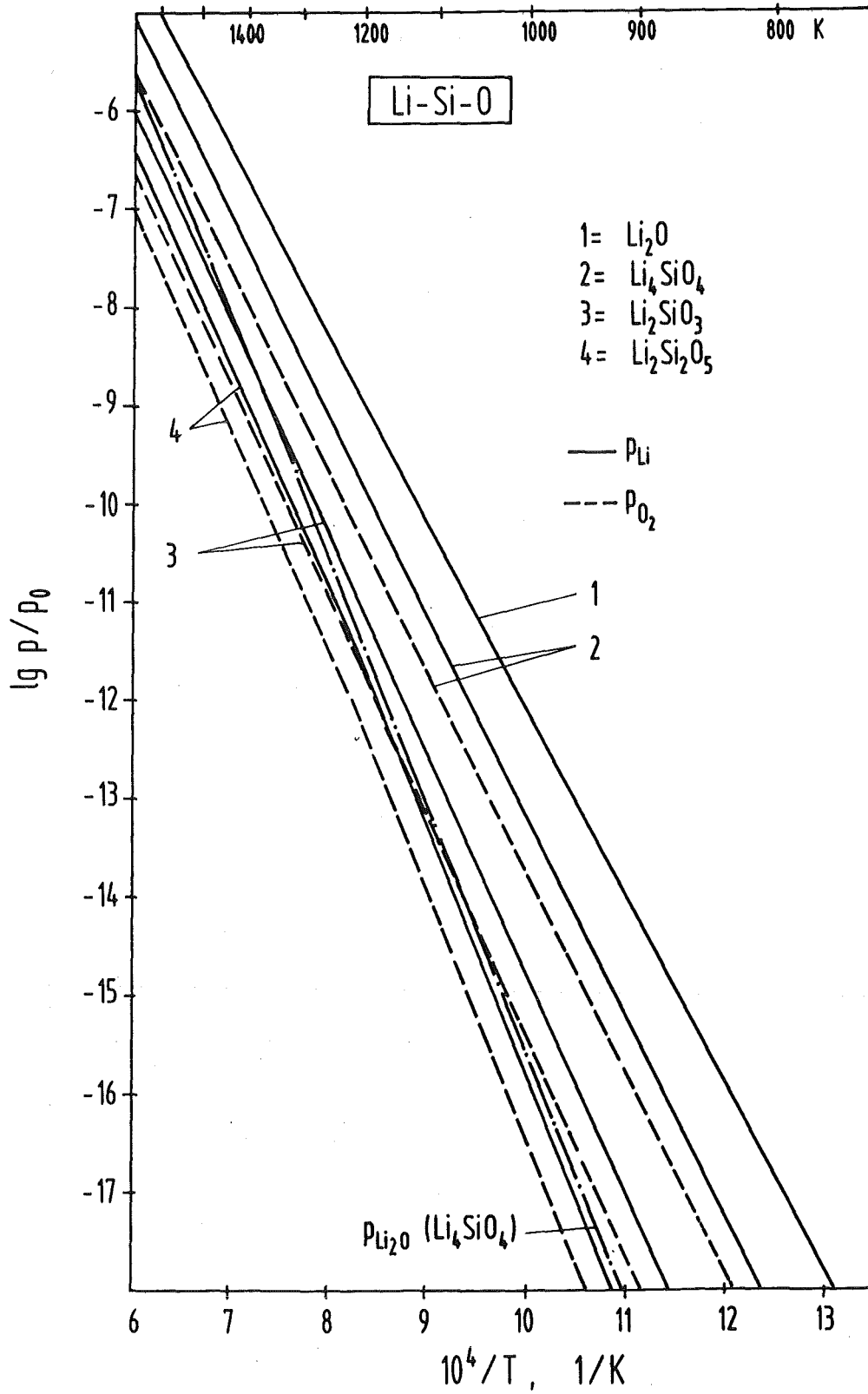


Fig.12: Dissociation pressures of lithium and oxygen over lithium compounds in the Li-Si-O system. $p_0 = 1 \text{ atm} \hat{=} 101325 \text{ Pa}$.

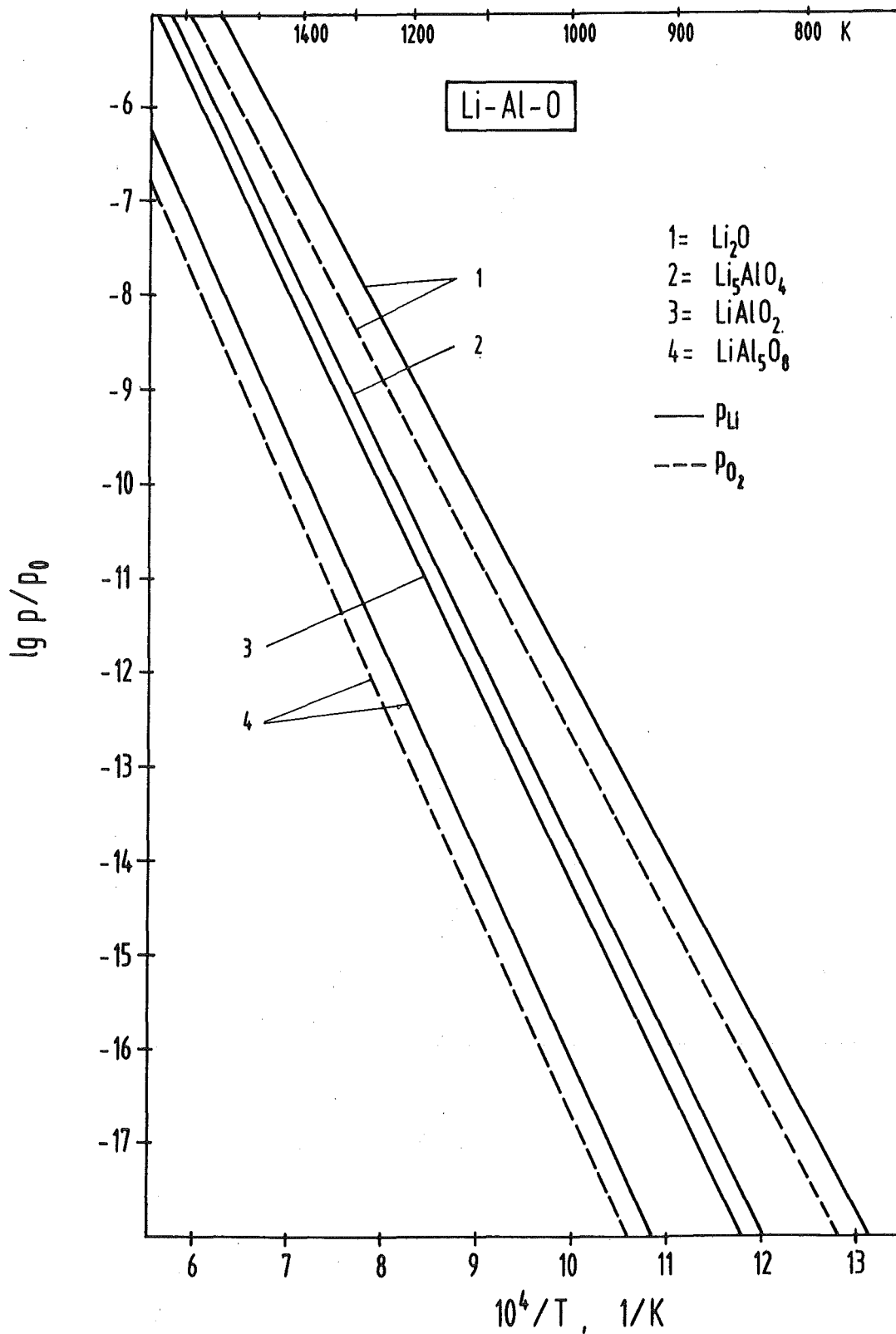


Fig. 13: Dissociation pressures of lithium and oxygen over lithium compounds in the Li-Al-O system. $p_0 = 1 \text{ atm} \hat{=} 101325 \text{ Pa}$.

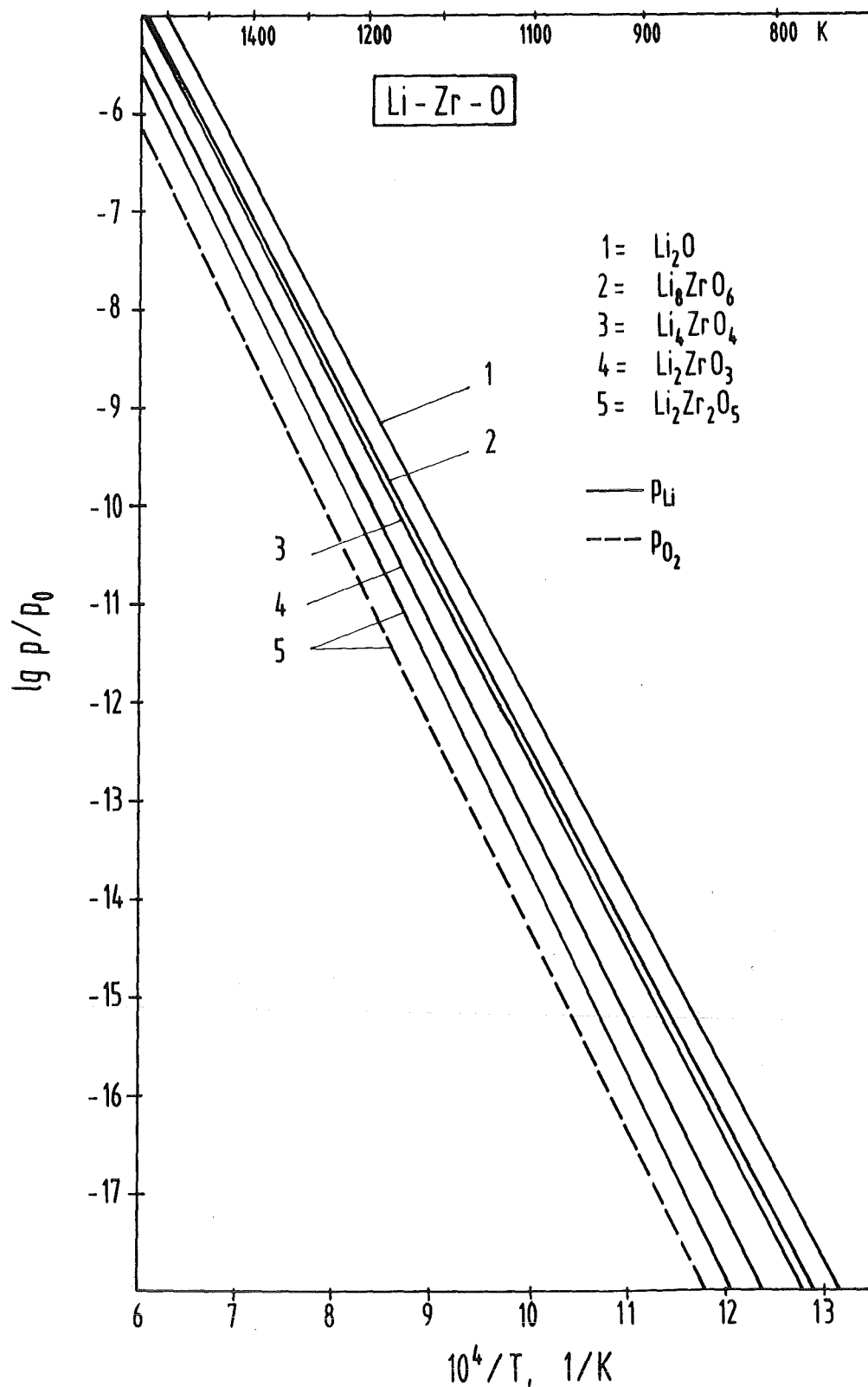


Fig. 14: Dissociation pressures of lithium and oxygen over lithium compounds in the Li-Zr-O system. $p_0 = 1 \text{ atm} = 101325 \text{ Pa}$.

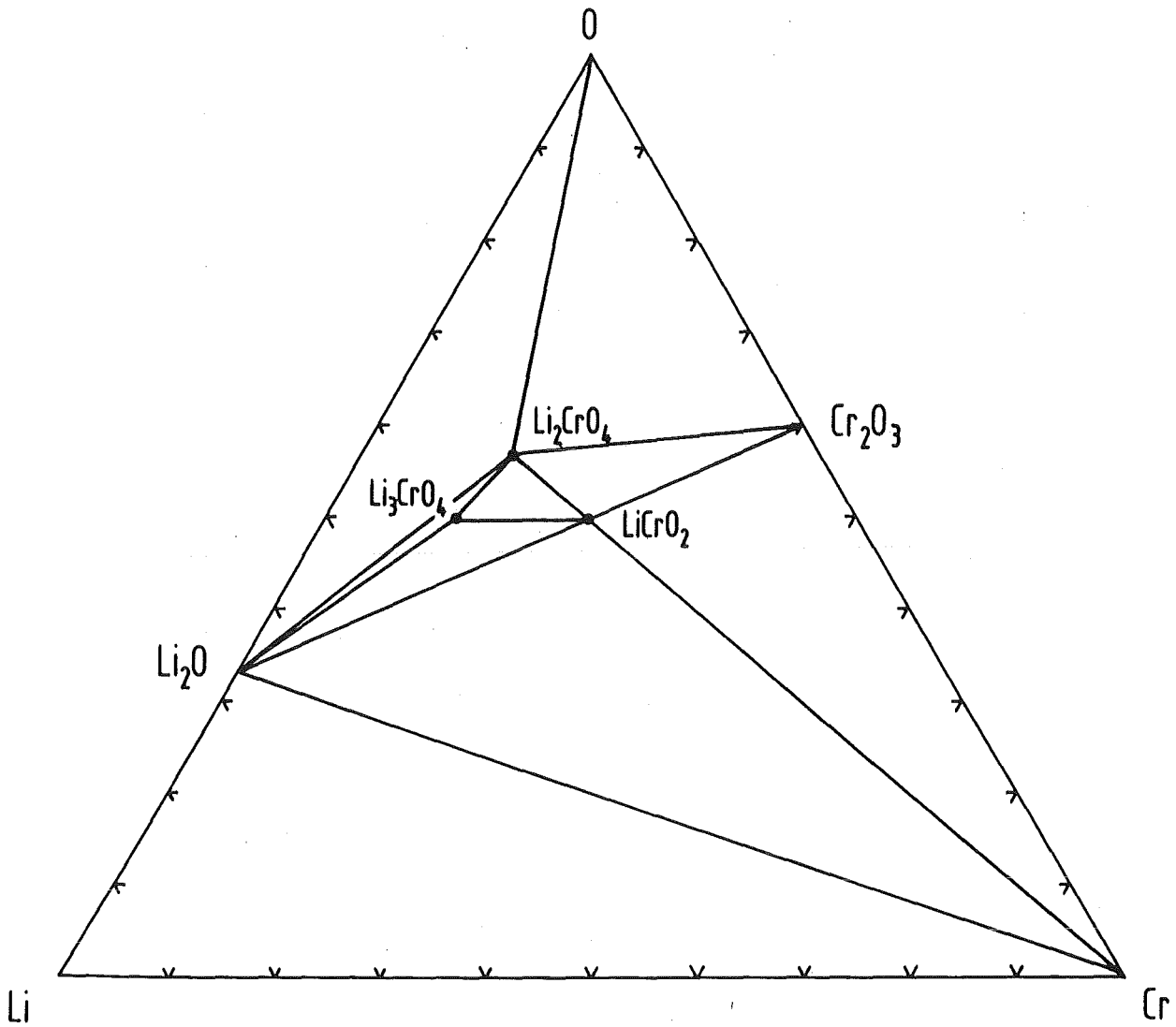
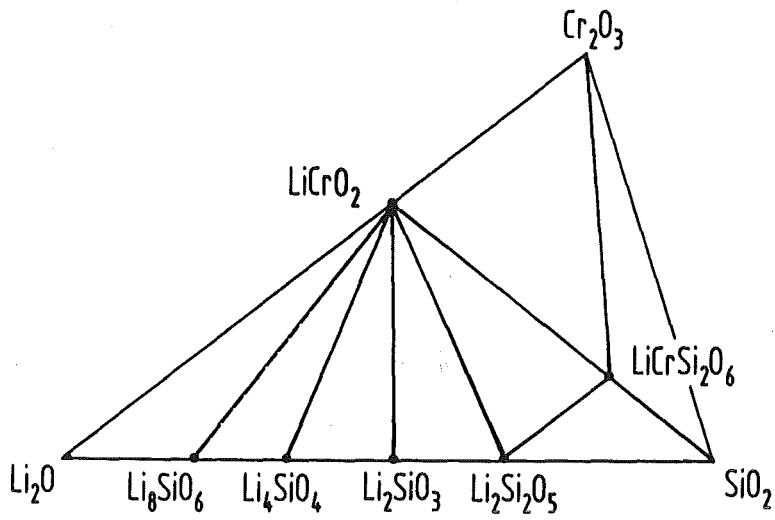


Fig. 15: Phase diagram of the Li-Cr-O system and cross section level $\text{Li}_2\text{O}-\text{Cr}_2\text{O}_3-\text{SiO}_2$ for the quaternary Cr-Li-Si-O system for 600 to 1200K.

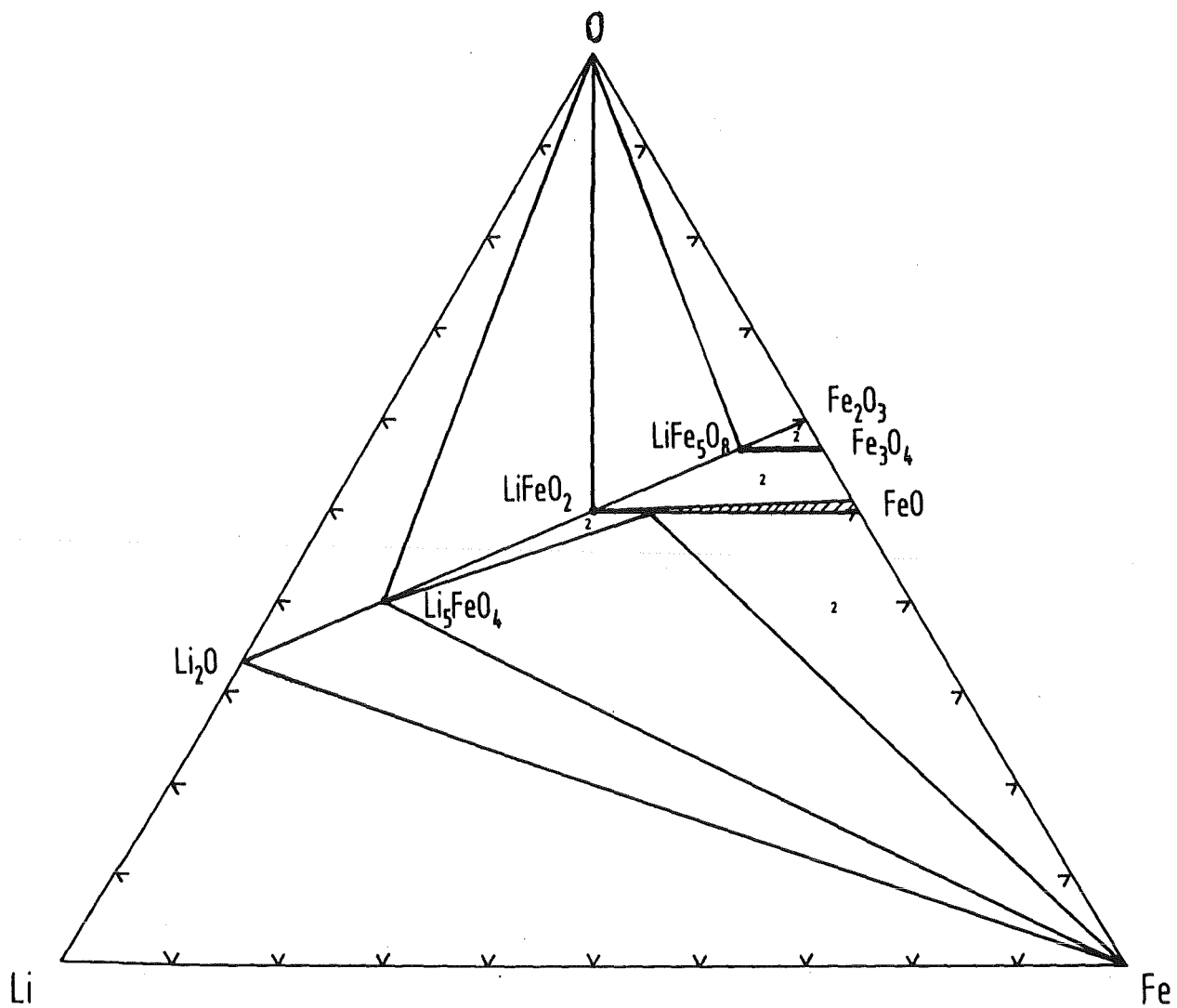
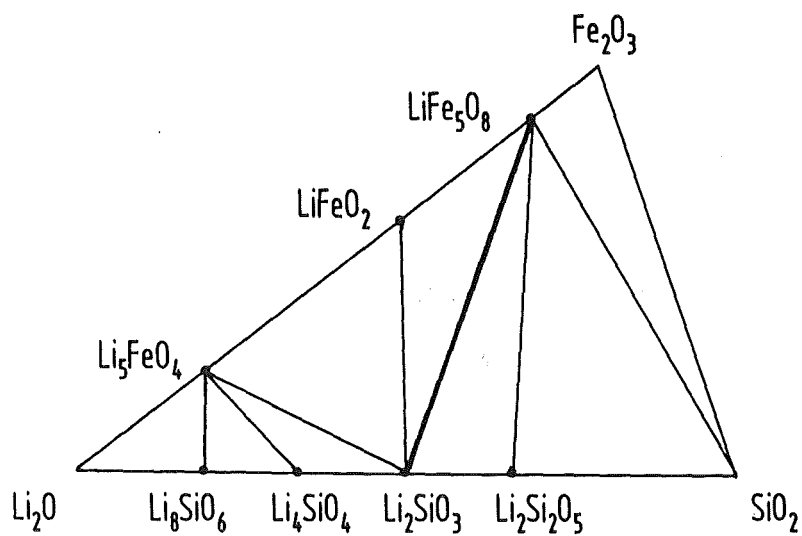


Fig. 16: Phase diagram of the Li-Fe-O system and cross section level $\text{Li}_2\text{O}-\text{Fe}_2\text{O}_3-\text{SiO}_2$ for the quaternary Fe-Li-Si-O system for 600 to 1200 K.

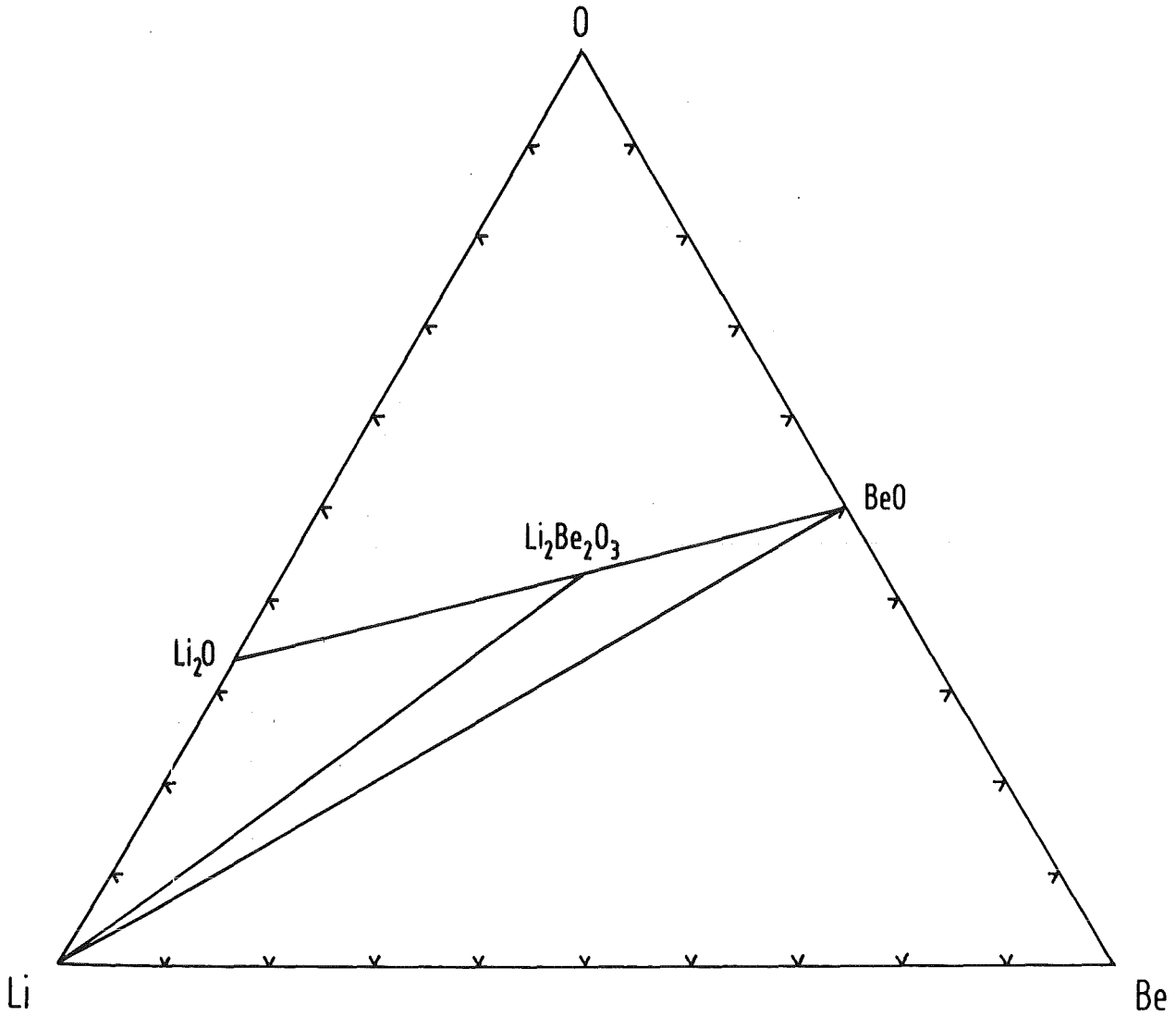
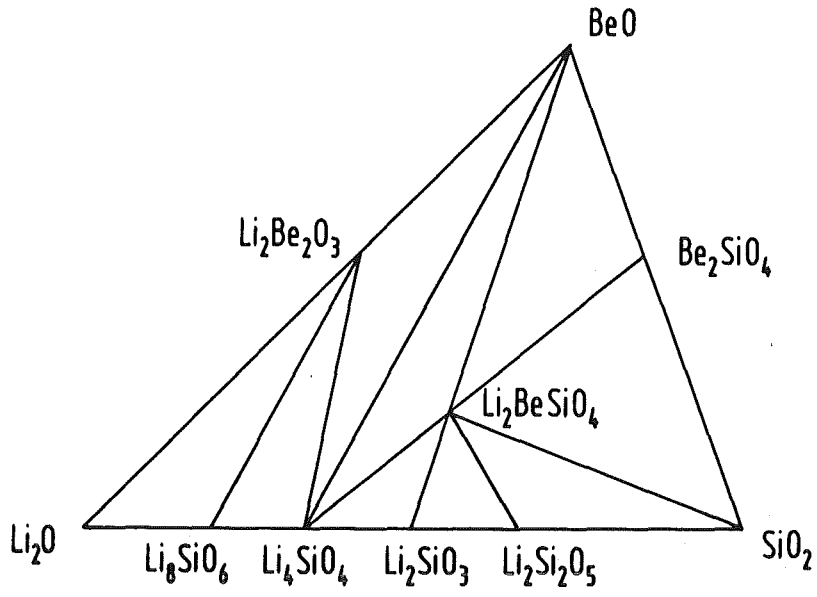


Fig. 17: Phase diagram of the Li - Be - O system and cross section level Li_2O - BeO - SiO_2 for the quaternary Be - Li - Si - O system for 600 to 1200 K.

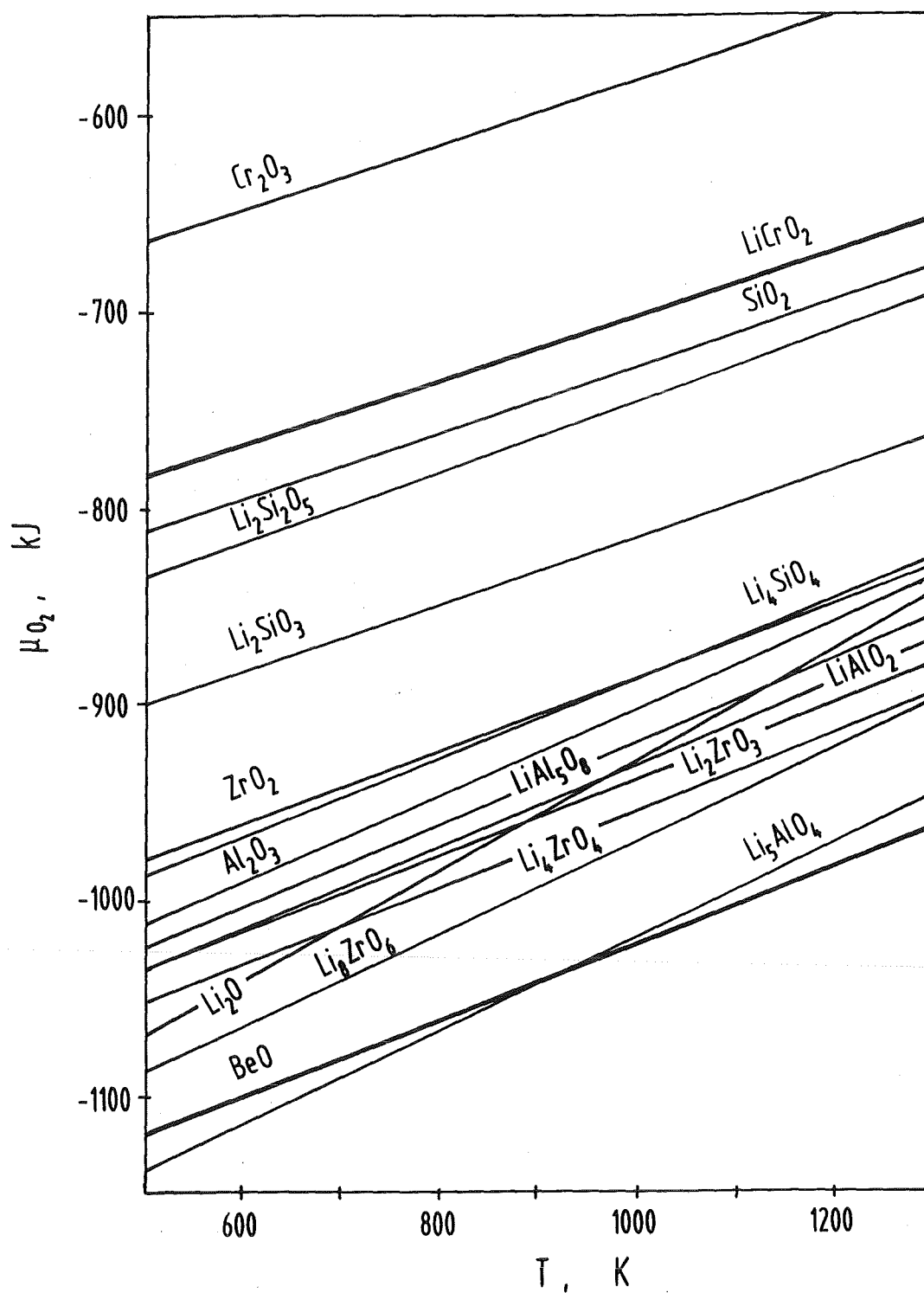


Fig. 18: Oxygen potential of formation of ceramic compounds.

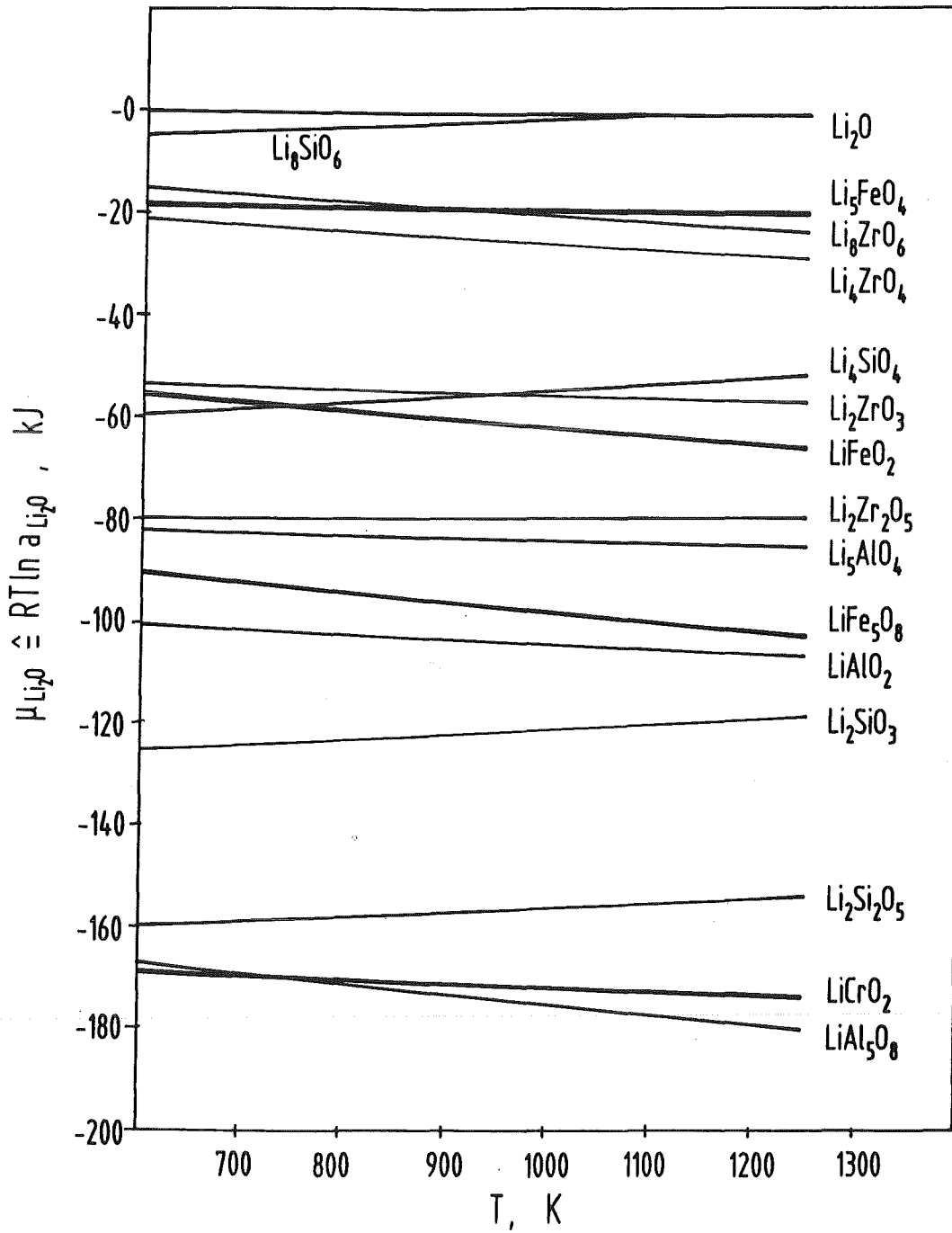


Fig. 19: Potential of Li_2O of ceramic materials